Passivation of Gallium Arsenide Nanowires for Solar Cells:

A thesis presented for the degree of
Master of Physics

Austin Irish

LUND UNIVERSITY

Department of Physics
Division of Solid State Physics

Supervisors:
Magnus Borgström
Stephanie Essig

Project duration: 8 months
May 6, 2019

Acknowledgements

Throughout this project I have grown a lot as an independent researcher. Despite the large amount of individual work that was put into this thesis, the help I received from others was extremely beneficial and instructive.

First and foremost, I would like to thank my primary supervisor, Magnus Borgström. From the very first day we met, his alacrity and his wisdom have been truly indispensable. Without his constant support, both institutional and personal, I could not have accomplished anything. I am deeply grateful. Similarly, I would like to thank Arkady Yartsev and Stephanie Essig who acted as co-advisors. Though my interactions with them were not daily, their assistance at critical moments was absolutely essential. It is only because of their decades of experience and timely support that I even had a project.

Next, I would like to thank Xianshao Zou and Enrique Barrigon. While doing work in their respective departments (Chemical Physics and Solid-State Physics), they played an invaluable role in my day-to-day success. They are indefatigable. Whether it was coming into the lab on evenings and weekends, or giving patient guidance during their busiest moments, their insight and dedication to research are simply unquestionable. I owe them much more than my gratitude.

Lastly, I would like to thank a group of wonderful people who gave me generous support, often on short notice. Particularly helpful were: David Alcer, Pavel Chabera, Lukas Hrachowina, Guy Koeckelberghs, Anders Kvennefors, Chuanshuai Li, Ebbe Nordlander, Ergang Wang, Xulu Zeng and Yuwei Zhang. They are perfect examples of the kind and dedicated people who make Lund University such a friendly and successful institution.

Abstract

A strategic and diverse set of passivation methods for gallium arsenide nanowires was studied. Using a time-resolved photoluminescence setup at 100 K and 300 K, the radiative recombination of charge carriers was resolved on a picosecond time scale. Characterization of these nanowire arrays on their native substrates provided reliable and nondisruptive measurements of thousands of nanowires simultaneously.

Three promising passivation methods were explored yielding unexpected results. First, an international collaboration was created which identified poly(3-[3,7-dimethyl-octyloxy] thiophene) (P3OOT) as a novel, conjugated polymer-based passivation material. Results were inconclusive. Second, an established hydrazine-sulfide solution treatment was compared with a low temperature, low vacuum plasma nitridation technique. The hydrazine treatment unexpectedly demonstrated depassivation whereas the plasma method strongly exceeded expectations. These measurements of plasma treated gallium arsenide nanowires may be the first publicly documented evidence for passivation using this procedure.

Overall, the results of these experiments further demonstrate the strong need for passivation of GaAs nanowires and proposes a new and relatively simple nitrogen plasma method which partially achieves this goal.

Contents

List of Initialisms

AlGaAs aluminum gallium arsenide

AlN aluminum nitride

ALD atomic layer deposition

AsH_3 arsine

CCD charge-coupled device

CVD chemical vapor deposition

Chalmers Chalmers University/Chalmers tekniska högskola

EBIC electron-beam-induced current

GaAs gallium arsenide

GaN gallium nitride

HCl hydrogen chloride

HOMO highest occupied molecular orbital

KU Leuven Catholic University of Leuven/Katholieke Universiteit Leuven

LUMO lowest unoccupied molecular orbital

MOVPE metal-organic vapor phase epitaxy

MBE molecular-beam epitaxy

NW nanowire

P3OOT poly(3-[3,7-dimethyl-octyloxy]thiophene)

PL photoluminescence spectroscopy

SEM scanning electron microscope

SSPL steady-state photoluminescence spectroscopy

TMGa trimethylgallium

TRPL time-resolved photoluminescence spectroscopy

QY photoluminescence quantum yield spectroscopy

Chapter 1

Introduction

1.1 Motivation

According to The Fifth Assessment Report of the United Nations' Intergovernmental Panel on Climate Change, anthropogenic fossil fuel emissions are the primary cause of the highest atmospheric greenhouse gas concentrations since well before the existence of modern humans.[1, 2] It has also been well established that "continued emissions of greenhouse gases will cause further warming and... limiting climate change will require substantial and sustained reductions of greenhouse gas emissions."[1] Particularly troubling, is that increased global warming does not just harm humans now. Elevated temperatures increase the "likelihood of severe, pervasive and irreversible impacts" which may persist for centuries even after fossil fuel emissions cease. [1, 3] Given the uncertain and mixed international commitment to replacing fossil fuels [4], it is more important than ever to find ways to make renewable energies like solar more attractive. This can either be done by decreasing cost or increasing efficiency. This research considers both.

Manufacturing costs shrink as production volumes increase. Into the future, an increasingly important consideration for global solar energy production will be efficiency.[5, 6] Whereas the first generation of solar energy production took advantage of mature silicon technology, and the second generation reduced costs by thinning devices, the third generation seeks to keep efficiencies high while maintaining thin films of cheap material. This has been done by increasing the efficiency of cheap architectures like all-polymer cells, and by reducing the costs of high-efficiency (eg. III-V) semiconductor devices. One way to reduce III-V (eg. GaAs, InP etc.) production cost is simply to use less material. NWs have the ability to absorb sunlight from beyond their physical cross-section and their better absorption properties allow them to use only a fraction of the material of a comparable thin film.[7, 8] Though this is beneficial, the more significant advantage of nanowires is the possibility for heteroepitaxy. Epitaxial growth of III-V semiconductors like GaAs is usually done on a larger piece of the same type of expensive material, ie. homoepitaxy. Unlike thin-films, nanowires, because of their small size, can be grown on different and cheaper substrates despite having different atomic spacing. A second way to reduce cost for high efficiency materials like GaAs is to reimagine the growth process. At Lund University, a novel, high-volume, substrate-less growing method called Aerotaxy was discovered. With this method, epitaxial growth happens midair as a stream of seed particles move through carefully controlled gases in a growth chamber.[9, 10]

Such advanced techniques still suffer from imperfections due to our incomplete understanding of how NWs form and function. An especially significant cause of reduced

efficiency is due to an intrinsic feature of nanoscale physics, surface-to-volume ratio. As volume shrinks, surface area becomes relatively large. Accordingly, bulk, thin films and nanostructures of identical materials will each have different properties.[11] Surface inhomogeneities and defects, for example, will have a much larger influence on nanostructures. Because of this unique property, if nanostructured devices are to succeed, vexatious surfaces must be passivated. That is, their surfaces must be tightly controlled so that efficiency remains high.

1.2 Background

1.2.1 Passivation

A typical architecture for the nanowires studied in this research is shown in Figure 1.1a. Put simply, incident sunlight with energy greater than the bandgap of GaAs can be absorbed. This creates excited electron-hole pairs. Careful doping in the NWs generates an electric field, which separates charges and pulls them to the tops and bottoms which are connected to metal contacts. These contacts are then connected to a circuit as part of a functioning device. However, that is for an idealized, properly functioning device. One of the most significant challenges in making GaAs nanowires successful in photovoltaics is controlling their charge dynamics. It is here that nanowire surfaces pose a major challenge.

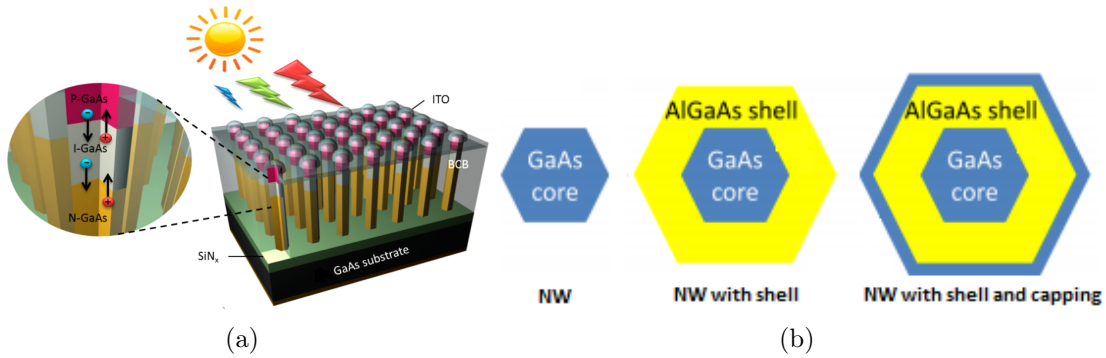

Figure 1.1: a) Arrayed GaAs nanowires in a p-i-n junction solar cell. Sunlight is absorbed by nanowires which creates electron-hole pairs. *p*- and *n*-type doping creates electric fields which guide the charges toward collection at the nanowire ends where electrical contacts connect to a circuit for use. Adapted from Yao et al.[12] b) Top view of a passivated nanowire. Epitaxially growing a shell of AlGaAs provides electrical passivation and a cap of oxidizing GaAs provides chemical passivation. Adapted from Joyce et al.[13].

Gallium arsenide is known to have the right fundamental properties for photovoltaics (eg. high-mobility, semiconducting, direct 1.42 eV bandgap etc.), but when it comes to actual operation, performance is often severely degraded. A fundamental reason for this is that, unlike silicon, it lacks a stable, electrically passivating oxide. Furthermore, surface-to-volume ratio increases with decreasing size. In the same way children get colder than adults, a nanowire shaped like the support column of a building will 'feel' like it has a surface approximately one million times larger. For films and bulk material this is not as significant, but for nanowires a surface is never far away. Joyce et al. estimated that excited electrons might "sample nearly the entire volume of the nanowire during their lifetime."[14]

At nanowire surfaces, trapped charges and midgap states strongly affect performance.[15, 16] So does recombination.[17, 18] Any charges that recombine before exiting the nanowire cannot be utilized and are wasted energy. Surface phenomena like dangling bonds, defects, strain, surface reconstructions and bonding to other materials (eg. oxygen) can create midgap states that otherwise would not exist (consider Figure 1.2). If these states reduce charge mobility or allow recombination, they can diminish critical device performance characteristics like open-circuit voltage and short-circuit current.[11, 14, 19, 20, 21, 22, 23] Thus, passivation is the name given to the process of improving surfaces and ameliorating these deleterious occurrences.

Passivation is usually thought of in two ways, electrical passivation and chemical passivation. In electrical passivation, the active material, which has desirable and homogeneous properties within the volume, must have its surface treated in such a way that its functionality is not diminished. For GaAs, the oxide that naturally forms on the surface, and sometimes even the intrinsic surface itself, is well-known to interfere significantly with device performance.[11, 24, 25, 26, 27, 28] In chemical passivation, the material must be stable and isolated from its environment. For example, it should not degrade or change composition (influx, outflux or rearrangement of material) over time and under expected operating conditions. In this sense, it can be thought of as a protection. An effective but difficult method is shown in Figure 1.1b. An expitaxial shell of AlGaAs provides electrical passivation and capping with GaAs provides chemical passivation.

1.2.2 Gallium Nitride

Nitrogen-based passivation of gallium arsenide goes back decades.[25, 26, 29, 30, 31, 32, 33] Nitrides in general (eg. Si_3N_4, AlN), and GaN specifically, are obvious materials to study because of their wide bandgaps and their chemical and thermal stability. (Si_3N_4 for example, was used as a mask for the growth of the nanowires studied in this research.)

A wide bandgap material bonded to a surface can provide electrical passivation. It is useful when a type-I (straddling gap) heterojunction is formed (see Figure 1.2a) because electrons and holes become energetically confined to the nanowire. This is probably the case for a GaN/GaAs-NW heterostructure but the known literature appears to be inconclusive.[34, 35] In order to illustrate the effect, Figure 1.2b shows a system with known band offset which demonstrates the principle.

Epitaxial capping with a larger bandgap semiconductor is an established passivation method used in many circumstances. When growing conditions are simpler or manufacturing costs pose a smaller constraint (eg. small volume, undoped or thin film growth; aerospace or military contracts) it can be very effective.[13, 16, 37, 38] For burgeoning mass-production processes like Aerotaxy, growth dynamics are not fully understood and complexities like doping can be difficult to control. Therefore, easier to control, non-epitaxial alternatives like nitridation are being sought.[11, 30, 39, 40, 41, 42]

Wet Chemistry: Hydrazine-Sulfide Solution

One way of converting the of surface GaAs to GaN is with wet chemistry. Passivation of GaAs with sulfur-based solutions (eg. ammonium sulfide, sodium sulfide) are effective and well-established procedures. Unfortunately, the sulfide surface lacks stability, and similar to epitaxial AlGaAs shell-growth, requires the use of additional coatings to keep the surface intact. This makes nitrogen-based solutions more attractive.

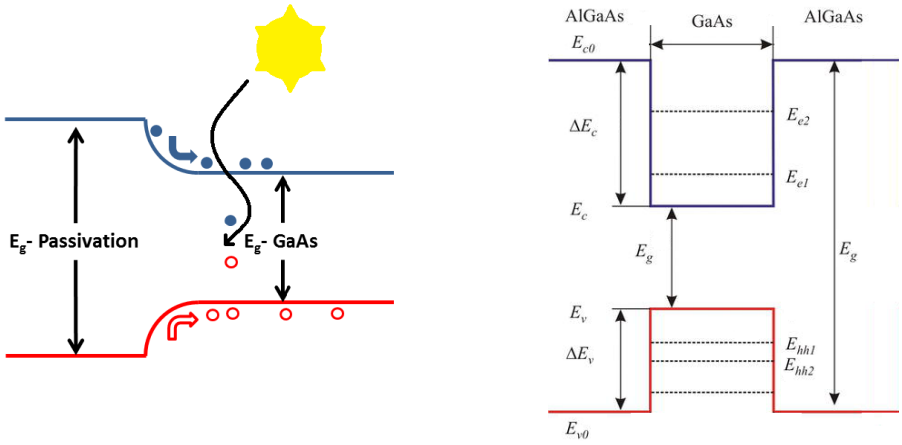

(a) (b)

Figure 1.2: Ideal band alignment between a GaAs-NW surface and a passivating shell. a) Generic band structure for any wide bandgap material providing a potential barrier, confining charges to the nanowire. b) AlGaAs/GaAs/AlGaAs quantum well structure representing an idealized case used in epitaxial passivation. Adapted from Demyanenko et al.[36] This band offset, combined with the possibility for lattice matching, is the primary motivation behind in-situ MOVPE shell growth shown in Figure 1.1b.

On GaAs substrates, Berkovits and Ulin pioneered a procedure using a hydrazine solution that effectively converts GaAs(100) surfaces to GaN.[41, 42] Since then, they have extensively published about the process. Most importantly, they have reported on hydrazine's ability to create an ultra-thin, stable, passivating layer of GaN. They have not only attempted to characterize the chemical reactions taking place, but they have also discovered the process's crystal surface and pH dependency, and provided an explanation for its passivating influence.[43, 44, 45, 46, 47, 48, 49, 50, 51] Most recently, they even demonstrated its potential for passivating GaAs nanowires enclosed by {110} facets.[11] That was the impetus for this project.

The hydrazine-sulfide solution's chemistry proceeds as follows. The nanowires studied in this research were grown on arsenic-terminated (111)B substrates; see Figure 1.3a for a useful visual aid. In order to 'clean' the surface, oxides must be removed to expose As. The solution reported by Berkovits et al. contains a mixture of hydrazine and sodium sulfide and is highly basic. During the initial phase of the reaction, anions quickly remove the oxidized surface. Once exposed to the solution, the surface-terminating arsenic can be removed due to the inclusion of a small amount of sodium sulfide (0.01 M). SH- anions combine with the As and desorb into the solution, leaving behind a bare Ga-terminated surface. Lastly, OH and N_2H_3 competitively attach to dangling Ga bonds. Importantly, though OH concentrations are much greater, N_2H_3 forms much more stable single bonds which can irreversibly form double or triple bonds with free neighboring Ga atoms.[49, 50] After only minutes, the self-limiting process ends and a monolayer of GaN is formed.

Figure 1.3b shows the photoluminescence intensity increase in GaAs NWs observed by Berkovits et al.[11] Their room temperature, stable, solution-based method for passivating nanowires was taken as a starting place for further research in this project. Because no other publications had verified their results, corroboration seemed warranted. Furthermore, an expansion of understanding was sought. Several of the research groups in and around Lund University use GaAs nanowires but also including dopants. It is an open

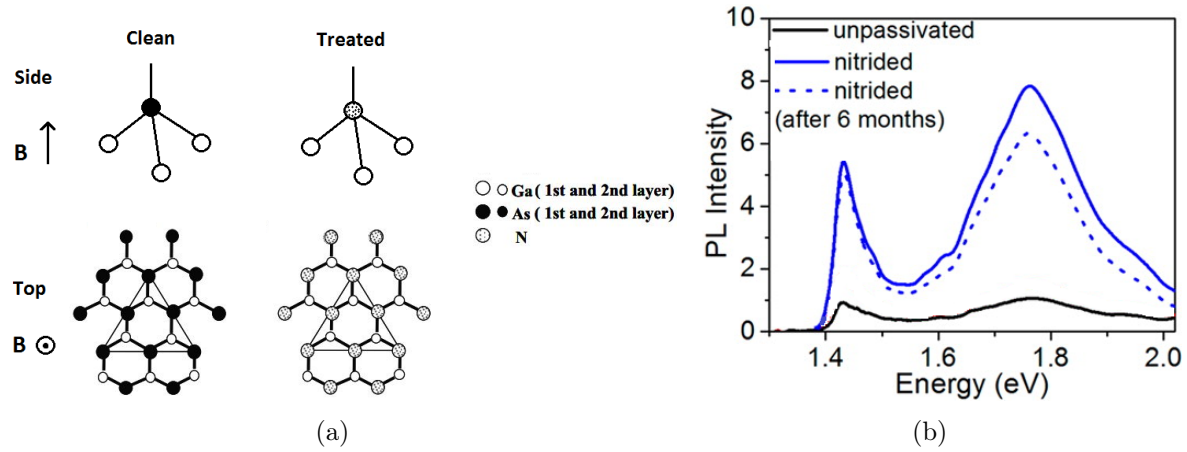

(a) (b)

Figure 1.3: Modification of GaAs(111)B crystal surface by hydrazine solution. a) The basic solution cleans the surface by removing the oxide. Next, SH- anions from the sodium sulfide remove surface As and open a site for nitrogen to attach. Finally, nitrogen molecules from hydrazine become multiply and irreversibly bonded to the surface Ga. b) Observed photoluminescence intensity increase due to nitridation with hydrazine (even after six months), demonstrating both electrical and chemical passivation. Adapted from Berkovits et al.[11, 43]

question what influence hydrazine-modified surfaces will have on the doped nanowires used in their photovoltaic structures. Additionally, steady state photoluminescence is a limited measurement and more sophisticated techniques like time-resolved photoluminescence were assumed capable of providing much more information about carrier dynamics which could be useful for subsequent development of solar devices. Thus, this hydrazine-sulfide solution was identified as a fruitful method for further research.

Nitrogen Plasma

An alternative to wet chemical nitridation is plasma-based nitridation. Simpler than most other methods (eg. ALD, CVD, MBE, MOVPE etc.), plasma methods can be done in situ, without precursors, and at relatively low temperature and pressure.[52, 53, 54] This makes it an attractive and potentially useful technique for application to nanowires. Numerous groups have reported on the theory and success of using nitrogen plasma to passivate GaAs electronic devices for at least three decades.[15, 26, 29] While some of these groups used only nitrogen, other groups included hydrogen, argon and ammonia.[29, 30, 33] After carefully considering the feasibility of these methods, the parameters published by Losurdo et al. were used as a starting point for this project.[39, 40, 55, 56, 57]

Losurdo et al. reported a 97% N_2 - 3% H_2 remote plasma method for creating an ultra thin (∼5 Å) layer of GaN on GaAs(100) surfaces. There is general agreement that the observed midgap states that exist on oxidized GaAs(110) surfaces is due to excess arsenic. This is likely due to free As, As_{Ga} anti-site defects, and As_2O_3.[14, 29, 58, 59, 60] Losurdo et al. systematically compared nitrogen-based plasmas and found that adding just 3% H_2 (by flow rate) provided a better, As-free surface than pure N_2 and NH_3.[30] Their optimized process involved a wet chemical preclean with HCl and a brief H_2 plasma pre-etch. Importantly, their process utilized a remote plasma setup that only allowed neutral atoms and radicals to impinge upon the surface, minimizing damage that can be caused by ion bombardment. This was a configuration replicated by other groups as well.[15, 32, 61]

As outlined by Capasso and Williams, the addition of hydrogen to the plasma is necessary for three processes[29]:

$$As_2O_3 + 12H \rightarrow 3H_20 + 2AsH_3$$
$$As + 3H \rightarrow AsH_3$$
$$Ga_2O_3 + 4H \rightarrow Ga_2O + 3H_20$$

Via these reaction pathways, surface impurities desorb and a clean Ga-rich surface is exposed to nitrogen radicals. Wet chemical precleaning prepares dirty samples for the process and a quick preetching with H_2 plasma removes the remaining oxide. A small fraction of hydrogen prevents oxide formation and free As from accumulating during the plasma nitridation of the exposed Ga surface. The last two steps are done at elevated temperatures to promote desorption.

As can be seen in Figure 1.4, the effect of this process on GaAs(100) substrates was substantial and reported by Losurdo et al. At room temperature, the PL intensity of the substrate was more than doubled. At low temperature, the difference between treatments was by more than an order of magnitude. In addition to this evidence for electrical passivation, the procedure displayed success with chemical passivation. After exposure to ambient air for $\sim 10^3$ days, PL intensity remained high and XPS was unable to detect any oxides.[40]

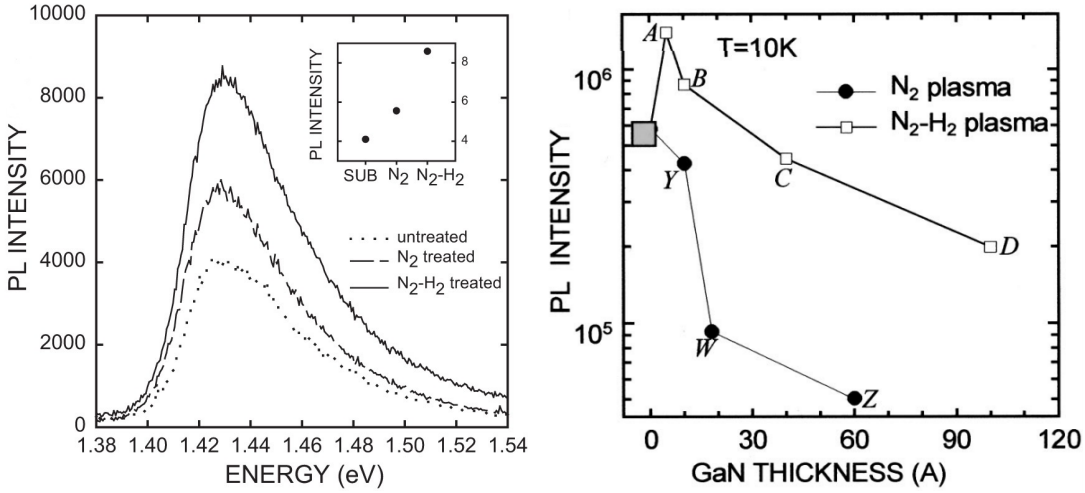

(a) (b)

Figure 1.4: Photoluminescence intensity measurements of undoped GaAs(100) substrates treated with N_2 and N_2-H_2 plasma. a) Emission intensity vs. photon energy at room temperature for various treatments b) Emission intensity vs. nitride thickness at 10 K for various treatments. Images have been modified from Losurdo et al. [39, 40]

Despite the apparent utility of this procedure, further investigation was needed. First, the only optical measurements published were of steady state photoluminescence. Second, only intrinsic GaAs(100) substrates were studied, not bulk (110) nor nanowire surfaces. It was clear that more could be learned about plasma nitridation especially for application to nanowire-based photovoltaics.

1.2.3 Conjugated Polymer

Theory

A much different, complex and relatively unexplored area of semiconductor surface passivation is with polymer-based methods. This is especially true when it comes to nanowire-based photovoltaics. In general, polymer-based photovoltaics have several desirable characteristics. Often made from abundant and non-toxic materials, they can also be lightweight, mechanically flexible, solution-processable and fabricated roll-to-roll.[62, 63, 64] This makes them extremely cheap and versatile, constituting an important part of the third generation solar cells.

Conjugated polymers have found significant use in solar cells, but this is often in purely organic or bulk heterojunction designs.[62, 65, 66] The possibility for using a conjugated polymer to passivate GaAs nanowire surfaces was promulgated by Yong et al.[24] They proposed a HOMO-level-dependent electron doping theory. Their XPS measurements and calculations of GaAs NWs found surfaces with a Fermi level midgap at $E_F \approx 5.1\,\text{eV}$. A useful visual aid can be seen in Figure 1.5a and b. When GaAs NW surfaces are cleaned and exposed to the loosely bound π-electrons from conjugated polymers, their lower energy surface states will fill (see Figure 1.5b). As their research suggests, GaAs(110) surfaces are highly electron deficient. Therefore, electron injection might passivate these states and prolong the radiative lifetime of charge carriers (see Figure 1.6).

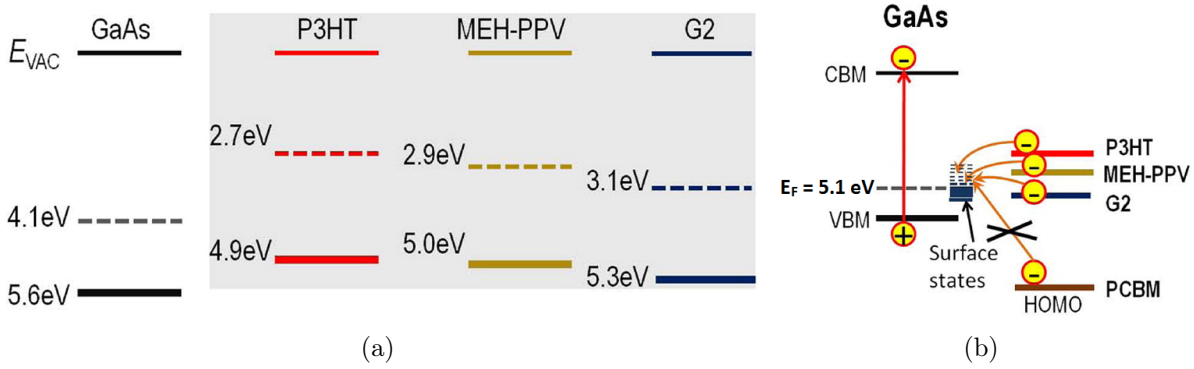

Figure 1.5: Band diagrams of GaAs and conjugated polymers. a) Dashed lines represent conduction/LUMO levels and solid lines represent valence/HOMO levels. b) Only if the polymer's HOMO level is higher than the midgap surface states of GaAs will electrons be injected into the nanowire. Adapted from Yong et al.[24]

According to the exponential trend in increased lifetimes observed by Yong et al. shown in Figure 1.6, even a modest change in polymer HOMO level could have a tremendous impact on recombination. In fact, their trend implies something nearly unbelievable. A conjugated polymer with an ionization potential just 0.2 eV smaller would extend carrier lifetime another order of magnitude right up to the nanosecond bulk limit ($\sim 10^{-9}$ s).[13, 14, 16, 18, 67] This extension seems improbable. One reason is that midgap states are discrete and might not spread throughout the entire bandgap. At some point the HOMO level, even within the GaAs bandgap, may lie significantly above all midgap states and therefore saturation would occur. It is even possible that P3HT already does this. Another reason would be if electron-deficient states are not the only cause of charge trapping and non-radiative recombination. If strain, defects etc. cause non-radiative recombination but cannot be saturated, electron injection will not passivate such features. Other exceptions

could exist as well. Nonetheless, such a dramatic and simple observation is notable and worth exploring.

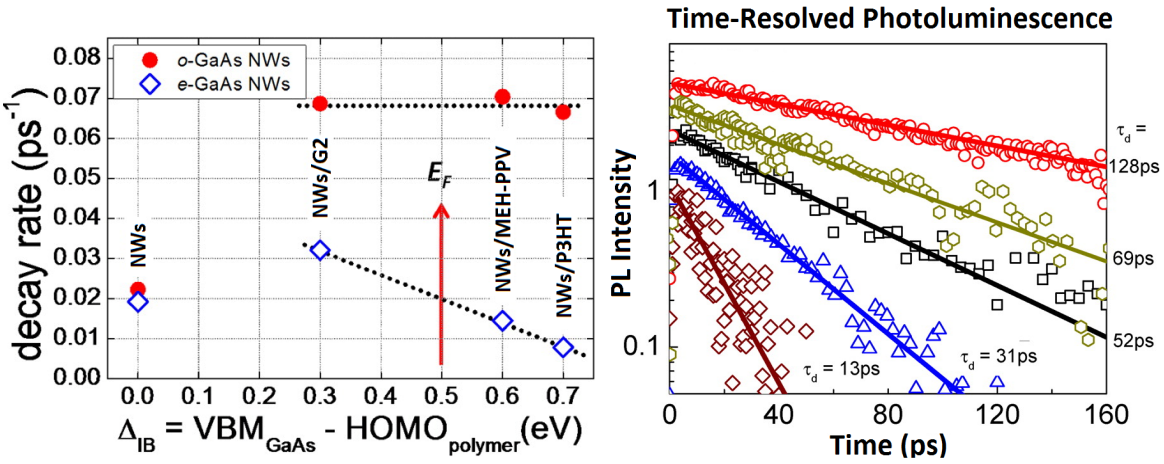

(a) (b)

Figure 1.6: Observed trend between polymer HOMO level and carrier lifetime in GaAs NWs. a) Red dots indicate oxidized NWs and blue diamonds represent NWs etched with 1M HCl. b) Red: P3HT, gold: MEH-PPV, black: NWs, blue: G2, brown: PCBM. As both plots show, increasing HOMO level above GaAs midgap states (−5.1 eV) prolongs radiative recombination. Adapted from Yong et al. [24]

Overall, this direction of research seemed promising for several reasons. Not only does it expand an architecture for cheap, easily-processed solar cells, but it also provides a model which can guide the synthesis of newer, better polymers. This idea, therefore, was the impetus for this part of the project. If a suitable polymer could be found, the HOMO-level-dependent electron doping model of passivation could be either substantiated or questioned. A material performing even better than P3HT might gain wide application.

Search for Suitable Polymer

With this in mind, a list of properties was identified for selecting a desirable polymer. It included: π-conjugation, chemical stability, electrically and optically nondistruptive, conformal, uniform, $-4.9\,\text{eV} < \text{HOMO} < -4.1\,\text{eV}$, easy to process, and refractive index less than GaAs nanowires.

After discussions with Dr. Wang from Chalmers University of Technology (Chalmers) and Dr. Koeckelberghs[1] from the Catholic University of Leuven (KU Leuven) a novel polymer was identified as having potential for nanowire passivation (see Figures 1.7a-d for a molecular description). Poly(3-[3,7-dimethyl-octyloxy]thiophene)[2] is in the class of exciting thiophene polymers that contributed to the Nobel Prize in Chemistry in 2000.[68] P3OOTs, are conjugated polymers which tend to have a HOMO level around −4.5 eV and bandgap about 1.9 eV[69, 70, 71].

Koeckelberghs et al. at KU Leuven have developed a method for synthesizing their P3OOT such that the monomers are strongly oriented head-to-tail (HT) ie. it is highly

[1]Dr. Koeckelberghs generously donated several grams of solid polymer for this research

[2]Though imprecise, for ease of communication poly(3-[3,7-dimethyl-octyloxy]thiophene) will be referred to by the name of the class of polymers to which it belongs, P3OOT, for the remainder of this thesis.

regioregular. Regioregularity is an important characteristic of conjugated polymers influencing everything from carrier mobility and HOMO level, to stacking and photon absorption.[71, 72] The benefit of using such a highly regioregular polymer is that it meets several of the most important characteristics identified earlier: conjugation, HOMO level, processability, stacking and uniformity.[72, 73, 74] Meeting the most important criteria, HT-poly(3-[3,7-dimethyl-octyloxy]thiophene) was therefore selected for the goal of passivating GaAs-NW{110} facets by the mechanism reported by Yong et al.

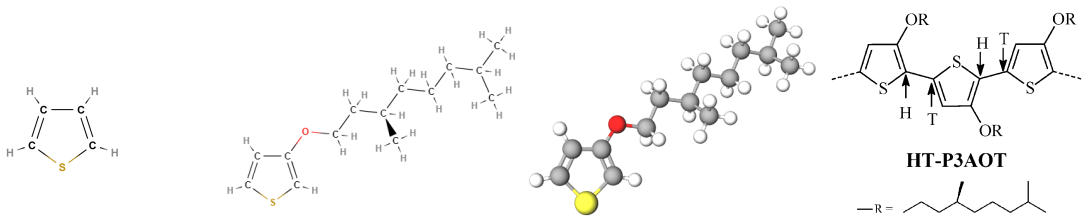

(a) (b) (c) (d)

Figure 1.7: Thiophene-based molecules, the sub-units of P3OOT. a) Simple thiophene monomer, b) P3OOT Lewis-Kekulé structure, c) P3OOT ball-and-stick model, d) regioregular, head-to-tail orientation of P3OOT

1.2.4 Characterization

As described in Section 1.2.1, passivation is a broad term encompassing several ideas (eg. environmental stability and electrical performance). It cannot be directly measured; instead, a material's properties are measured. Numerous methods can be used depending on the tools available and the properties of interest. They include: current-voltage measurements, steady-state and time-resolved photoluminescence spectroscopy (SS/TRPL), pump-probe spectroscopy, electron-beam-induced current, cathodoluminescence spectroscopy, photoluminescence quantum yield (QY) etc. Spectroscopic methods are useful, in part, because they can characterize intrinsic NWs without creating full devices. Three available techniques in Lund University's Chemical Physics department are QY, SSPL and TRPL. TRPL was selected because of its ability to acquire both intensity and time-domain information.

TRPL can be one of the most effective methods for evaluating the opto-electronic properties of nanowires. Offering a balance between complexity and diagnostic power, TRPL measurements are taken on the order of hours, despite being able to provide sophisticated information about the properties of a material. Easier measurements like SSPL are much faster and can be done with simpler equipment but cannot give time dependent information about radiative recombination. Conversely, pump-probe measurements like transient absorption spectroscopy offer very detailed information, but at the expense of ease-of-use and understanding. Therefore, for this project, it was decided that time-resolved photoluminescence was the appropriate technique.

Lastly, the use of spectroscopy to characterize passivation operates under the following conception. Within the semiconductor's bandgap, there should either be no states (intrinsic), or precisely controlled states (doped). Device operation critically depends on this. If midgap states exist it becomes energetically favorable for charges to leave the conduction band. Events like scattering, trapping of charges and non-radiative recom-

bination are more likely to occur. In a solar cell device if charges recombine quickly or their motion is impaired they are less likely to be collected and used by the circuit. Fewer charges collected means reduced efficiency. Band edge, radiative recombination is therefore inversely related to the prevalence of undesirable, non-radiating midgap states. Because different events quench radiative recombination in different, characteristic ways, the ability to resolve nanowire emission over time is an extremely fruitful method for evaluating passivation.[14, 20, 38, 75, 76, 77, 78] In other words, all excited charges will eventually relax, but they can do this in many ways. If the only process is radiative, when an excited electron and hole happen to meet, this can take an entire nanosecond. However, if the material has defects or impurities, charges may encounter midgap states in mere picoseconds, recombining non-radiatively. Thus, the intensity of NW emission and the lifetime of radiative decay are correlated with passivation, and comparing the rates of radiative decay provides a direct comparison of optoelectric quality of the material (the faster decay the lower the quality).

Alternatively, it can be thought of by analogy with global warming and the greenhouse effect. Earth's analog would be a nanowire. The earth, just like a nanowire, absorbs sunlight and its temperature increases. In a NW solar cell, this light gets converted into mobile charges whereas on earth, the electromagnetic energy re-radiates back into the atmosphere. Passivation thus can be thought of as the greenhouse gases that contain this energy within the system. Traps, defects and midgap states are equivalent to carbon-sinks like the oceans, forests and outer space (passivating materials). The analogy should only be taken lightly of course. As described in the introduction (section 1.3), greenhouses gas emissions are at dangerous levels and must cease. Passivation, on the other hand, will contribute to renewable energy production and a safer, more habitable planet.

1.3 This Work

Ultimately, the goal of this thesis was to propose and identify useful passivation methods in an attempt to improve GaAs nanowire surfaces. In order to achieve this, a thorough review of literature and theory was done. After careful consideration, two themes and several procedures were selected and subsequently studied.

The nitridation theme was chosen because of its history of success in similar applications. In theory, it works by saturating dangling bonds and removing midgap states that trap charges and/or allow recombination. Gallium nitride is a highly stable material with a wide bandgap which can both protect NWs and improve charge carrier lifetimes by removing inefficiency-causing midgap surface states. Two methods were considered in an attempt to convert the surface of GaAs nanowires to GaN. One uses a hydrazine-sulfide solution, and one uses a nitrogen plasma. A benefit of nitridation-based passivation is that it is more understood and has a well-substantiated theory. Its weakness lies in its increased complexity and cost compared to simpler methods like polymeric coating.

The polymer theme was chosen because of its greater potential. In theory, it works not by bonding to the crystal, but by saturating midgap surfaces states that trap charges and/or quench radiative recombination. It does this when the surfaces are in close contact and the band energies are carefully tuned such that loosely bound π-electrons in the HOMO of the polymer prefer the lower lying midgap states on the GaAs nanowire surface. Though significantly less substantiated, it represents a novel, cheap, and easy-to-produce method for passivating GaAs nanostructures. Ideally, it would combine the high quality optoelectronic properties of inorganic GaAs with high-volume processing methods like

roll-to-roll or Aerotaxy, all while increasing efficiency.

This aim of this research was broad. In general, it was to learn more about the properties of advanced photovoltaics, specifically GaAs nanowires used for solar cells. In particular, regarding hydrazine there was an attempt to either corroborate or contradict the narrow space it occupied in scientific literature. In addition to that, several aspects of this research can be considered supplementary to the existing publications. This research not only introduces time-resolved and temperature-dependent characterization, it includes measurements of nanowire arrays. Regarding plasma-based nitridation, an attempt was made to demonstrate its first-ever (to the author's knowledge) passivation of GaAs nanowires. Previously, neither GaAs(110) nor nanowire surfaces had been reported on. Finally, a very different, polymer-based passivation method was explored. International collaborations were made in order to study a novel, conjugated polymer and contribute to a relatively unexplored method of passivation. This project purposefully covered a wide range of passivation techniques with the two-fold goal of learning about photovoltaics, and finding cheap, easy methods of passivating GaAs NWs for the next generation of high-efficiency solar devices.

Chapter 2

Methods

2.1 Experimental Methods

2.1.1 Time-Resolved Photoluminescence Spectroscopy

Time-resolved photoluminescence is a sophisticated spectroscopic technique used to study the optoelectronic properties of materials. In a very simplified way, it is like steady-state photoluminescence after the laser has been turned off. After a pulse of excitation, emission (over a range of wavelengths) is recorded over time. Concomitant with its increased complexity, comes more detailed information. Understanding time-resolved photoluminescence requires a basic understanding of what happens both inside the equipment and inside the material. Consider the following description, aided by Figure 2.1. Measurement-specific details will be described alongside their respective experiments.

The pump and pulse lasers were manufactured by Spectra Physics. At Figure 2.1a1 a Millennia Pro E3383 laser used a neodymium-doped yttrium orthovanadate crystal (Nd:YVO_4) to produce up to 10 W of 532 nm continuous-wave laser light. This was used to pump a Ti:Sapphire crystal in a Tsunami 3960 pulsed laser unit (see Figure 2.1a2). Once mode-locking was achieved, the 800 nm, femtosecond pulses went to a Photop TP-2000 harmonic generator shown in Figure 2.1a3. Those pulses, then at 400 nm, were sent through a polarizer and focused onto the samples shown by Figure 2.1a4. The maximum power at the sample was 7.5 mW. After excitation, photoluminescence normal to the substrate traveled through a set of mirrors and a long pass filter (JB450) on the way to a Hamamatsu C6860 streak camera.

The emission collection setup operated as follows, see Figure 2.1b). A Chromex spectroscope separated photons horizontally (parallel to the ground) by wavelength on their way to a photocathode. The streak camera's photocathode generated electrons proportional to photons, which were then accelerated down the streak tube between a pair of sweeping electrodes. A time-varying potential was then swept between the electrodes, deflecting the electrons vertically over time and into a multichannel plate which increased the number of electrons by several orders of magnitude. The two-dimensionally- (wavelength and time) sorted electrons then impacted a phosphor screen. Lastly, the phosphor screen emitted photons which replicated the original pattern back into an image which could be collected and analyzed by a CCD.[79]

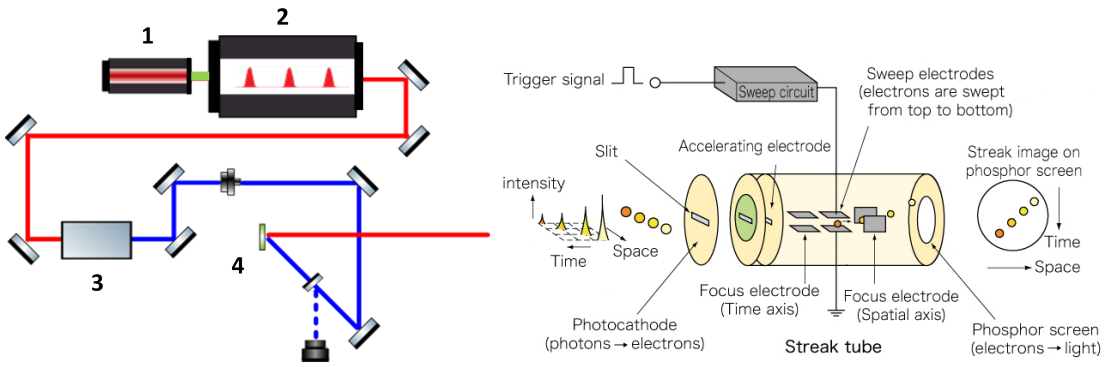

(a) (b)

Figure 2.1: Schematic of the setup. a) Top-view of the laser setup used for sample excitation: 1) Nd:YVO_4 continuous wave pump laser (1064 nm → 532 nm), 2) Ti:Sapphire pulse laser (780 nm), 3) harmonic generator (780 nm → 400 nm) and 4) sample and emission; folding mirror and power meter b) Schematic of the streak camera. In front of the streak camera was a spectroscope that sorted emission by wavelength. The sorted photons were converted to electrons by a photocathode. The electrons were deflected by a time-varying potential and multiplied by a multichannel plate. They then hit different vertical positions on a phosphor screen depending on when they entered the streak camera. After exiting the streak camera, a CCD collected the phosphor screen's photons and converted them to a digital signal. Diagram adapted from the Hamamatsu product manual.[79]

Measurements were collected at 100 K (using liquid nitrogen), 294 K (room temperature) or 300 K while samples were kept in a sealed N_2 environment. Generated pulses had a repetition rate of ≈ 80 MHz and were ≈ 100 fs long, leading to a temporal resolution of ≈ 4 ps (see appendix for support). For increased nanowire absorption, a harmonic generator was used to double the excitation frequency to 400 nm. A polarizer was also used to transverse-electrically polarize the light which impinged upon the sample at ≈ 55° from the NW axis. Reflectivity increases with angle. Accordingly, this is a common configuration for increasing substrate reflection and increasing relative nanowire emission.[20, 75]. The focused spot size was ≈ 110 µm in diameter, encompassing ≈ 1000 NWs. Excitation powers were varied on the order of mW which resulted in excitation intensities $\sim 10^5\,\mathrm{W\,m^{-2}}$. If all of the pulse's photons were absorbed and each photon excited only one electron, the resulting number of electron-hole pairs generated would be $\sim 10^{14}$ Hz per nanowire. The spectroscope was operated using a slit width of 150 and 50 grating lines/mm. Overall, the emission collection parameters were selected to increase precision and reduce signal from the substrate.

2.1.2 Nanowires

The gallium arsenide nanowires studied in this thesis were grown with a two-step, metal-organic vapor phase epitaxy (MOVPE) process. The GaAs(111)B growth substrates were highly p-doped ($\sim 10^{19}\,\mathrm{cm^{-3}}$) with zinc and purchased from AXT, Inc. Hexagonal arrays with pitch = 500 nm were patterned by nanoimprint lithography and etched into silicon nitride. Nanowire growth proceeded via the vapor-liquid-solid method from either evaporated or electroplated gold (due to laboratory changes). Using trimethylgallium (TMGa) and arsine (AsH_3) as precursors, a brief nucleation step was followed by annealing at elevated temperature (600 °C) and then a cooler, longer growth period (450 °C, 10 min). The general process is well described in literature and known to produce uniform, straight, zincblende nanowires.[80, 81] See Figure 2.2 for a visual reference.

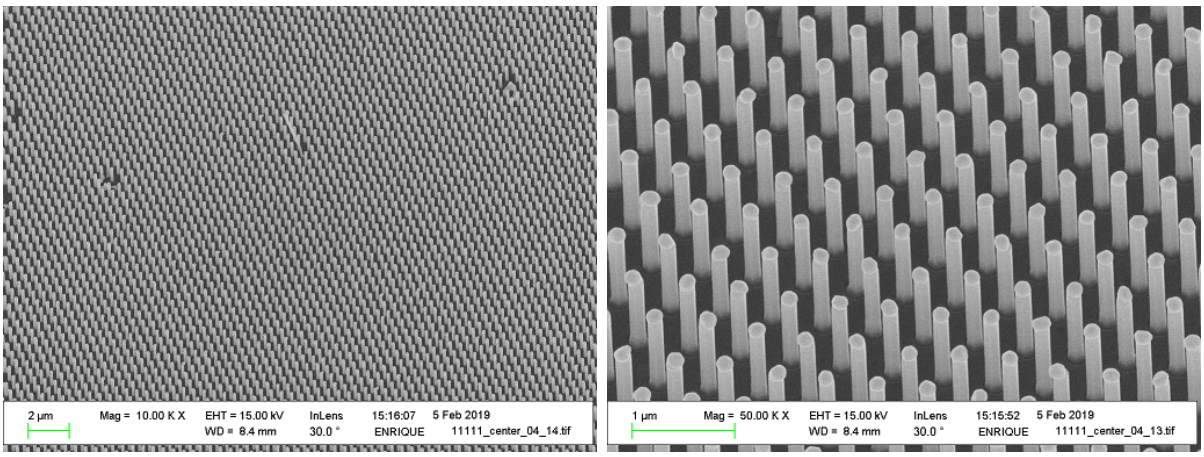

(a) (b)

Figure 2.2: SEM images of a nanowire array grown for this project. The approximate size and uniformity of these nanowires can be considered representative of all samples measured throughout the project. Images were taken at the sample's center with the following configuration: accelerating voltage = 15 kV, current = 30 µA, working distance = 8.4 mm, substrate tilt = 30° a) Approximately 3,500 nanowires shown at magnification = 10.000 x b) Approximately 150 nanowires shown at magnification = 50.000 x. Used with permission from Enrique Barrigon.

To the extent possible, nanowire growth conditions were kept the same throughout this project because the primary goal was to study surface passivation of the nanowires grown, not the growth itself. However, two growth parameters were purposefully varied at strategic moments. These were V/III ratio and high-temperature annealing.

V/III ratio is the ratio of the gas molar flow rate of the group V precursor (arsine) to the gas molar flow rate of the group III element (trimethylgallium). For two reasons it was decided that V/III ratio was a growth condition worth examining preliminarily. First, it would provide an opportunity to gain measuring experience. Second, prior to this project, carrier lifetimes in nanowires grown by established passivation methods had been limited. This prompted speculation that it was the internal properties of the nanowires that were the origin of short observed radiative lifetimes, not the surface passivation.[20] Since it is well established that gas molar flow rates strongly affect nanowire growth (eg. defect creation, crystal phase, morphology etc.), changing the V/III ratio was an opportunity to improve the internal properties of the nanowires before attempting to improve their surfaces.[14, 82, 83, 84, 85, 86, 87, 88]

The second condition varied was a post-growth, high-temperature anneal (750 °C, 1 min). It has been shown in published literature that with a similar growth procedure, annealing nanowires reconstructs their cross-section from a dodecagon to a hexagon.[81] Specifically, six {112} facets merge into six {110} facets. Since passivation is largely a question of surfaces, making the nanowire surfaces uniform seemed relevant to the research (for further justification see Section 3.5).

A list of all samples and their properties is given in Table 2.1 below (for SEM images see the Appendix) .

2.1.3 HCl Deoxidation

Removing the oxide from GaAs NW sample surfaces had two purposes throughout this thesis. First, GaAs NWs exposed to air can have such poor surfaces that at room tem-

Sample/Property	L ($\pm 0.1\,\mu m$)	D ($\pm 5\,nm$)	V/III Ratio	Anneal
10669[1]	1.0	160	105	×
10672[1]	2.4	160	66[2]	×
10673[1]	1.8	160	66[2]	×
11059	1.4	160	66[2]	×
11060	1.1	160	33	×
11061	0.8	160	13	×
11062	1.1	160	7[3]	×
11063	0.9	160	22[4]	×
11073	1.7	160	213[3]	×
11110	1.1	160	22[4]	×
11111	1.1	160	22[4]	✓

Table 2.1: Properties of nanowire samples and growing conditions. All pieces were $\leq 1\ cm^2$. [1]Due to laboratory changes, significant time elapsed during which no nanowires could be grown. During this period, older samples which had been grown under slightly different conditions were studied. [2]The established V/III ratio when this project began. [3]Unlike the other samples, in order to achieve such disparate V/III ratios both TMGa and AsH_3 flows had to be adjusted, not just AsH_3. [4]Justified further in Section 3.1, V/III ratio = 22 resulted in the best room temperature radiative lifetime and was therefore the parameter replicated for subsequent growth.

perature their emission is not even detectable.[89] In order to ensure emission detection and gain experience measuring with the TRPL setup, samples were generally deoxidized prior to measurement. Second, whenever it was necessary for a passivation treatment to directly interact with the GaAs nanowires' surfaces (ie. plasma and polymer methods), an HCl deoxidation treatment was used to remove the surface oxide immediately prior to the procedure.

The procedure used for deoxidation was the one implemented by Yong et al.[24] It is a simple and well established process. A 1 M concentration of hydrochloric acid was prepared (12:1 hydrochloric acid 37% to deionized water) and the samples were submerged for 30 s. The samples were then rinsed in deionized water for 10 s, carefully dried by N_2, and transferred to their next environment. Deoxidized NW arrays were always kept in N_2 during and after treatment to the extent possible with available equipment. Individual sample details are given along with their measurement results.

Overall, removing oxygen and other contaminants from the surface of nanowires is usually not sufficient for a well-functioning device however. Despite its efficacy for deoxidation, XPS measurements have shown the process does little to remove excess arsenic in the form of antisites and aggregates, and the post-treatment Fermi level of the NW surface remains largely unchanged.[24] Once the HCl exposes the surface however, that is when passivation treatments can be implemented.

2.1.4 Hydrazine

The hydrazine treatment developed by Berkovits et al. and used for this thesis should be replicated only using care.[11] The solution and its reactants (all purchased from Sigma-Aldrich) though safe if handled properly, are highly flammable and toxic. The passivating

solution was made by adding anhydrous hydrazine-dihydrochloride to hydrazine-hydrate until pH $\approx$ 8.5 is obtained. The solution starts out highly basic and adding the anhydrous powder lowers the pH. (Care should be taken not to lower the pH to 7; acidic solutions with hydrogen cations can produce toxic gas via $H^+ + SH^- \rightarrow H_2S$) Once at pH $\approx$ 8.5, 0.01 M sulfide was achieved by adding sodium sulfide nonahydrate (240 g/mol $\rightarrow$ 2.4 mg/mL for 0.01 M). Solutions were then heated with a hotplate and oil bath to 80 °C. The treatment itself only involved submerging the samples for 10 min, carefully rinsing with deionized water for 10 sec and drying with N_2. Despite literature reporting that the GaN surface created by this treatment needs no protection from ambient air, the samples were precautionarily kept in a sealed N_2 environment. For safety reasons, during these procedures limited users were allowed into the laboratory and the handling of all toxic chemicals was done by approved lab staff. Risk assessments were made, personal protective equipment was worn, and proper disposal and cleaning of materials was always practiced.

2.1.5 Plasma

The plasma nitridation process used in this research was guided by the procedure developed by Losurdo et al.[30, 40] It contains three steps: a wet chemical etch and H_2 plasma for the purpose of removing contaminants and exposing the bare NW surface, and a 97% N_2 - 3% H_2[1] plasma step to convert the surface from GaAs to GaN. Accordingly, all NW samples were deoxidized with wet chemistry prior to plasma nitridation. This was done by the HCl deoxidation procedure described in Section 2.1.3. Unlike the remote plasma MOVPE system used by Losurdo et al., the plasma system used for this thesis was a Fiji F200 ALD system designed by Cambridge NanoTech (see Figure 2.3). The operating principle is largely the same however. It uses an inductively coupled plasma source which is separated from the sample in the reaction chamber. This separation, called "remote-" or "downstream-" plasma, is essential for reducing damage to the sample caused by accelerated ions. By ensuring that only radicals (and other neutral species eg. H_2, Ar) reach the NW surfaces, the nitridation process is much gentler. This is especially consequential for nanowires.

The procedure used was as follows.[2] Within minutes of an HCl treatment the samples were quickly transferred to the plasma chamber and put in vacuum, P = 0.05 torr. Next, the chamber and sample were kept under vacuum for 30-120 min to remove any surface water. Then, the chuck and chamber were heated to 250 °C for the H_2 pre-etch. Gas flows were: $Ar_{carrier}$ = 40 sccm, Ar_{plasma} = 200 sccm, H_2 = 40 sccm. The plasma power was P = 300 W and exposure lasted only 3-12 s. Next, the conversion to GaN was done after another temperature increase, 350 °C. For this step the gas flows were $Ar_{carrier}$ = 20 sccm, N_2 = 133 sccm, H_2 = 4 sccm. The operating power was kept at P = 300 W and the plasma time varied between 10-40 s. Finally, the samples were allowed to cool to 150 °C before removal and were sealed in a vacuum environment. The entire process took about 5 h per sample with almost all of the time being spent on the initial wait under vacuum and the final wait during cooling. (For a discussion of this see Section 4.2.)

[1] For ease of communication 97% N_2 - 3% H_2 will sometimes be abbreviated to just N_2 throughout this thesis. A pure N_2 plasma was never used. Similarly, the word plasma will be used as a general term to describe this process and the radicals it created, despite the fact that ionized particles played little to no role in the process.

[2] For the exact recipe used see the Appendix or the tool recipe at LNL.

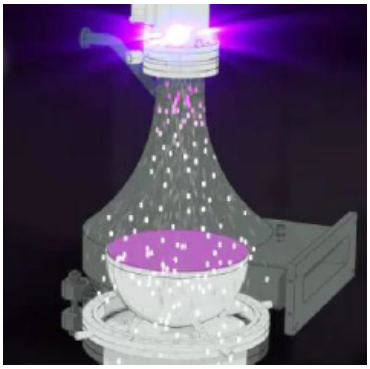

Figure 2.3: Equipment diagram of remote ICP plasma chamber with downstream sample chamber. Bright pink represents creation of plasma. Pink dots represent radicals (N, H). White dots represent inert carrier Ar gas. This remote configuration, with its associated lack of accelerated ion bombardment, is considered imperative for achieving minimal damage to NWs. Reproduced from Cambridge NanoTech Fiji F200 system manual.[90]

Very few details were published about the H_2 pre-etch procedure used by Losurdo et al. (eg. "a few seconds").[39] So, a full comparison cannot be made. Where unavailable, parameters were chosen in accordance with tool constraints and previously developed processes at the Lund Nano Lab. The primary differences between the Losurdo et al. nitridation treatment and the one used for this research were the plasma power and pressure. Losurdo et al. found an optimum with their procedure on GaAs(100) substrates at Power = 200 W and Pressure = 0.2 Torr. In order to achieve effective ignition of the N_2 plasma these parameters were slightly adjusted, though no significant effects are expected. Temperature, gas concentrations and exposure time were shown to play a much larger role and a comprehensive study of these parameters was outside the scope of this project.[30]

2.1.6 P3OOT

Poly(3-[3,7-dimethyl-octyloxy]thiophene) was considered for GaAs nanowire passivation because of its status as a high HOMO level conjugated polymer. With an estimated HOMO level at −4.5 eV, it should be able to saturate more midgap states than the lower HOMO level polymers studied by Yong et al.[24] Whenever reasonable, efforts were made to replicate their experimental procedure. Yong et al. drop-cast 30 µL of 0.2 mg/mL polymer in 1,2-dichlorobenzene onto their nanowires within an N_2 environment. This was followed by heating on a hotplate at 70 °C for 3 h. Once finished, samples could be measured with TRPL.

P3OOT is known to be soluble in 1,2-dichlorobenzene, chloroform and tetrahydrofuran. So for this project, all three solvents were examined (Sigma-Aldrich D56802, EMD Millipore 1.07024, and EMD Millipore 1.09731 respectively). Based on visual inspection[3], all three effectively dissolved P3OOT (at 0.2 mg/mL) with tetrahydrofuran being the fastest. Due to facility limitations, it was only possible to carry out the following procedures in a fume hood (not glove box). First, the solvent was measured and gently warmed (10 mL, 40 °C). Next, smaller pieces of polymer were carefully generated with a scalpel and measured with an electronic scale. After combining solvent and solute, thirty minutes were allowed to pass with occassional stirring. Next, NW array samples were

[3]P3OOT was only obtained toward the end of this project. Accordingly, a comprehensive understanding the polymer and how to apply it to nanowire arrays was out of the scope of this project. Recommendations for potential procedural improvements will be discussed in Section 4.2.

placed on a glass slide and the polymer solution was drop-cast by pipette; 30 µL was more than enough to cover the samples. Following deposition, slides and samples were heated on a hotplate at 70 °C for 3 h and then sealed in a N_2 environment.

For subsequent TRPL measurements, chloroform was the chosen solvent for three reasons; see Figure 2.4. First, its evaporated solution appeared to uniformly embed most of the nanowires; see Figure 2.4a. Second, it seemed to result in thin film coverage of the entire NW surface, Figure 2.4b. Third, it was the solvent used in published literature for thin film measurements.[91, 92, 93]

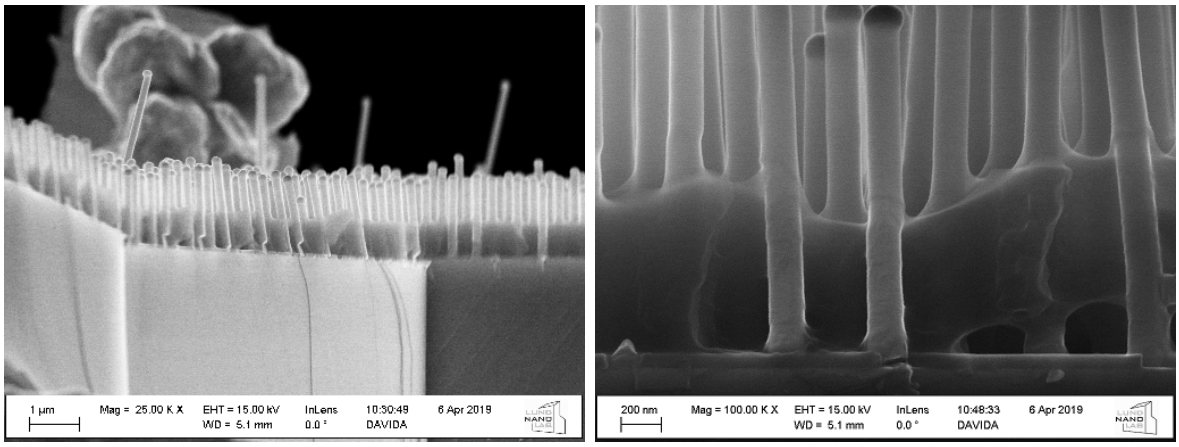

(a) (b)

Figure 2.4: SEM cross-section images of cleaved NW samples drop-cast with 0.2 mg/mL) P3OOT in chloroform. Images were taken with the following configuration: accelerating voltage = 15 kV, current = 30 µA, working distance = 5.1 mm a) Cross-section at 25,000x magnification showing P3OOT partially embedding the NW array. b) Cross-section at 100,000x magnification showing probable thin film (< 10 nm) coverage by polymer. Note the contact angle between polymer and nanowires, indicating adhesion. Also note the texture difference between the formerly covered nanowire surface and nanowire surface above the embedded layer. This was treated as evidence for a thin film coating.

2.2 Analysis

Measuring emission was only a small part of the process of producing data. For every measurement, background measurements with the laser off/blocked had to be made and subtracted from the data. In addition to that, shading measurements with a calibrated light source by Ocean Optics were conducted to account for wavelength-dependent features in the setup. These two were background signal subtracted which in the end resulted in data that was much more accurate.

For data analysis, HPDTA 9.1 and OriginPro 2019 were used. HPDTA was the software used both to collected the signal (controlling the spectrometer and streak camera) and to handle the raw data before importing into Origin. All plots were generated with OriginPro which has the ability to quickly organize large amounts of data and do mathematical functions like generating curve fits and integrating signal intensity.

Throughout this thesis many time-resolved emission plots were examined. In an attempt to characterize these in a consistent and meaningful way a working definition for photoluminescence lifetime was created. The definition, the amount of time between half-peak intensity during the rise in emission and the time at which emission intensity fell to a factor of $\frac{1}{e^2}$ of peak intensity, was formulated and used for two principal reasons.

First, peak intensity, which is a common point for starting the lifetime measurement, was often difficult to determine. This was a consequence of the poor emission observed by the nanowires at room temperature. With very little emission and high noise, comparing samples based on such an indeterminable notion was vexing. Second, lifetime was judged to be finished at $\frac{1}{e^2}$ of peak intensity for two reasons. $\frac{1}{e^2}$ represents a decrease in intensity by about one order of magnitude, a substantial reduction, and it also happened to be near the point at which the samples rate of decay shifted significantly. After $\frac{1}{e^2}$ a second slower decay dominated and the decay was out of the time range of the measurements. Furthermore, mixing these two regimes would be profoundly deceptively both conceptually and physically.

Considering the time-dependent exponential decay equations 2.1 and 2.2, one should not confuse lifetime with another time value, τ, which represents a characteristic decay rate of an exponential decay process. Most often this first concept was used because it provided more descriptive utility for the vast majority of the highly unpassivated samples measured. τ comes from the observation that photoluminescence often decays exponentially and can be modeled by one of the following equations. Most of the emission observed in this thesis contained second or higher order decays which can be difficult to characterize at the time range the streak camera was operated at (100 ps). It was a choice between accurately measuring the first-order or higher order decays and since the first-order decays dominate, the shortest time range was chosen.

$$I = A_1 e^{\frac{-t}{\tau}} + y_0 \tag{2.1}$$

$$I = A_1 e^{\frac{-t}{\tau_1}} + A_2 e^{\frac{-t}{\tau_2}} + y_0 \tag{2.2}$$

Chapter 3

Results and Discussion

3.1 V–III ratio

Before attempting to study potential passivation methods, it was clear that a brief test of nanowire growth conditions could be beneficial. It is well known that gas molar flow rates, in particular, the ratio between the group V and III elements, strongly affects epitaxial nanowire growth. V/III ratio can influence: NW growth rate, defect concentration (eg. stacking faults, twin planes, interstitials, antisites, vacancies etc), crystal phase (WZ, ZB) and morphology.[5, 14, 82, 83, 85, 86, 87][88] In particular, Joyce et al. found that "...nanowires grown at a high V/III ratio have an exciton lifetime over 50% shorter than nanowires grown at a low V/III ratio..."[84] Accordingly, an examination of the influence of V/III ratio on time-resolved photoluminescence was conducted.

After deliberation, it was decided to grow five nominally intrinsic (undoped) nanowire arrays. Their properties can be seen in Table 3.1. Sample 11059 was grown using standard growth parameters. Arsine flow was primarily used to adjust V/III ratio. Because gas flow controllers have limited ranges, only some of the samples could keep TMGa flow constant. For the most extreme ratios tested, both molar flows had to be shifted. Sample 11061 was not characterized due to its poor nucleation during nanowire growth.

V/III Ratio	**L** ($\pm 0.1\,\mu m$)	**D** ($\pm 5\,nm$)	**Sample**
213[3]	1.7	160	11073
66[1]	1.4	160	11059
33[2]	1.2	160	11060
22[2]	1.0	160	11063
13[2]	0.8	160	11061
7[3]	1.1	160	11062

Table 3.1: Properties of the nanowires grown for this measurement. [1]Standard ratio used for growth. [2]AsH_3 flow adjusted. [3]TMGa and AsH_3 flows adjusted due to limited mass flow controller range.

Before characterization, samples were deoxidized with hydrochloric acid as described in Section 2.1.3. This was done inside a portable glove box in which the samples were also sealed in their measuring chamber. After preparation, samples were illuminated with the setup described in Section 2.1.1 at power, P = 7.5 mW, wavelength = 400 nm, T = 297 K. Emission was averaged over 100 exposures collected at 1 s per exposures. Emission slices

were averaged across the peak intensity region at the GaAs bandgap (871 nm).

Figure 3.1 gives a broad view of the emission dynamics of the V/III ratio samples. Two notable observations could be made even while making these measurements. First, the emission intensity decayed very quickly, requiring use of the system's fastest measurement time range. Second, the emission intensity was very weak. Though not desirable for photovoltaics, this was expected (see Sections 1.2.4 and 2.1.3). To induce substantial emission, spectra were collected at the highest power the laser could deliver.

One of the easier to make observations about these measurements was that there were roughly three groups. The slowest decay in emission occurs from the V/III ratio = 22 sample. Then, the next three sample decays are comparable: V/III ratios = 33, 66, 213. Finally, the V/III ratio = 7 sample's emission decayed fastest. This can be seen even more clearly in Figure 3.2b.

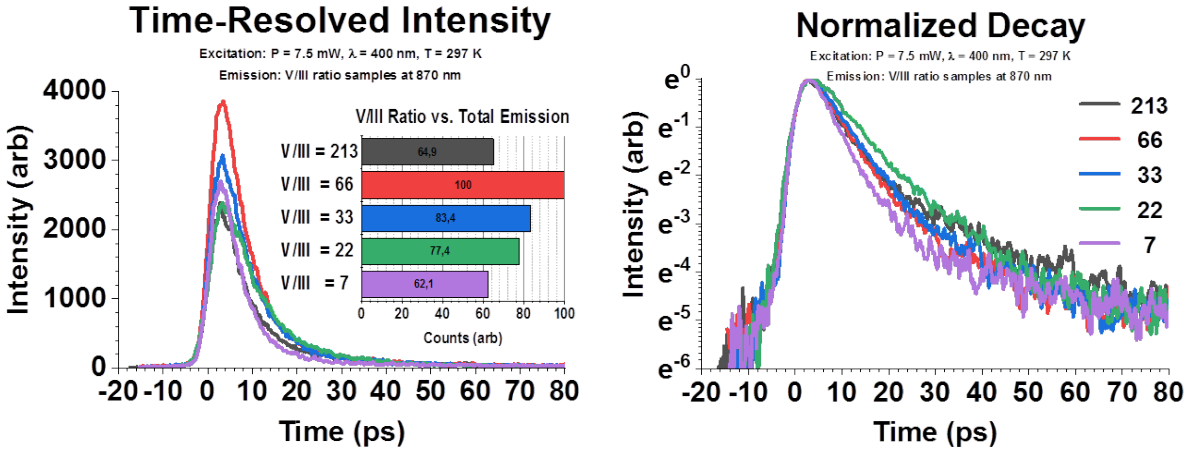

(a) (b)

Figure 3.1: Time-dependent photoemission intensity of nanowires grown with different V/III ratios. Curves show 100 ps of emission averaged across peak emission wavelength = 871 nm. To obtain a strong signal, excitation power was set near the system maximum at P = 7.5 mW. Excitation λ = 400 nm. Characterization T = 297 K a) Time-resolved intensity curves comparing their relative intensity. b) Normalized intensity curves showing relative decay rates across samples.

No discernable pattern was observed in connection with V/III ratio alone. Therefore, samples grown at V/III ratios = 66, 33 and 22 were examined more closely due to the fact that only one growth parameter had been changed, the arsine molar flow. It was here that a pattern emerged. Figure 3.2 shows a subset of the samples measured. Two clear trends emerged. The first related to intensity. When emission intensity was integrated over the entire time of collection (100 ps) it could be seen that V/III ratio was inversely related to total emission. The standard growth ratio, sixty-six, emitted the most, and the lowest ratio, twenty-two, emitted the least. At the present moment the cause of this trend is unclear, but it should be noted that intensity can change by orders of magnitude and these differences may not be a consequence of crystal quality changed by growing parameters. Instead, to name one example, it could be cause by a disparity between samples in the number of intact nanowires at the spot of the laser. Second, Figure 3.2b shows an observed trend between V/III ratio and photoluminescence lifetime. As V/III ratio decreases, lifetime increases. The nearly 25% increase is small relative to bulk GaAs lifetimes, but it in general agreement with the reports in literature motivating this experiment.[84] Excess arsine causes optoelectric degradation in GaAs.[58, 59] If

the crystallographic properties of these nanowires were changed by the factor of three reduction of arsine flow (for example reduced As antisites), then the improved lifetime of V/III = 22 might be a result of this change. Nonetheless, the overall intensity and decay of the NW emission was largely limited, probably due to the lack of passivation. Without further evidence available, this trend was taken as a justification for closer examination.

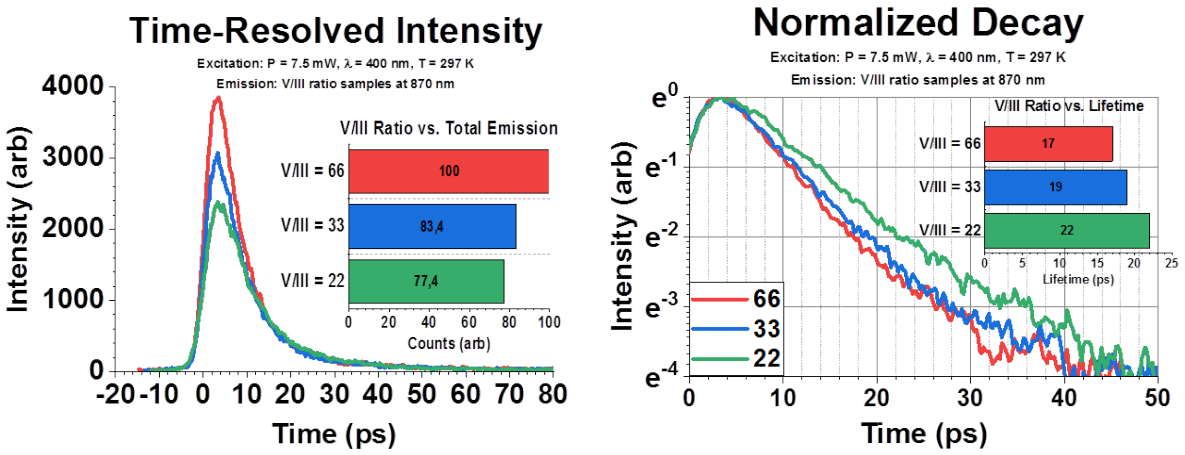

(a) (b)

Figure 3.2: Plots of a reduced sample set, representing a change in V/III ratio only due to changes in arsine flow. Note how the intensities and decays trend with V/III ratio. a) Time-resolved intensity curves at peak emission wavelength. Intensity increases with V/III ratio. b) Normalized intensity curves showing single exponential decay over the short time scale of tens of picoseconds. Note that lifetime increases as V/III ratio decreases.

Upon closer examination of all of the samples' decays, it was noted that all appeared biexponential (Figure 3.1b). Due to their weak luminescence and the limited time window of the measurements, a full characterization of the photoluminescence decay cannot be achieved. However, the curve fitting shown in Figure 3.3 strongly suggests biexponentiality, with at least two mechanisms reducing radiative recombination within the nanowires. One mechanism (or midgap state) appears to reduce recombination on the order of single picoseconds; the other was on the order of tens of picoseconds. The best curve to model the decay was $I = 1.7e^{\frac{-t}{8.5}} + 0.035e^{\frac{-t}{40}} + .0036$.

Figure 3.3 shows a typical exponential decay pattern observed and several things can be noted. The first-order decay of intensity appears linear on the logarithmic y-axis. However, over longer time scales (> 20 ps), there appears to be a second-order decay which is unresolvable at earlier times.

A few general observations can be made. First, the V/III ratio = 22 sample exhibited the longest lifetime. Second, it appears that simply raising/lowering the V/III ratio is not effect by itself. Significant deviations from the standard growth ratio did not result in the nanowire arrays with longest lifetimes. From these preliminary data, it was tentatively assumed that V/III ratio = 22 was a significant improvement over the current growth parameter.

One important thing to keep in mind however, is that these samples had only been treated with HCl to remove oxides; no passivation had been applied. So, although differences could be seen, all of these unpassivated lifetimes were short. As described in the Section 1.2.1, unpassivated GaAs NWs contain an prohibitive number of midgap states (due to dangling bonds, surface reconstruction, arsenic defects etc.) which prevent

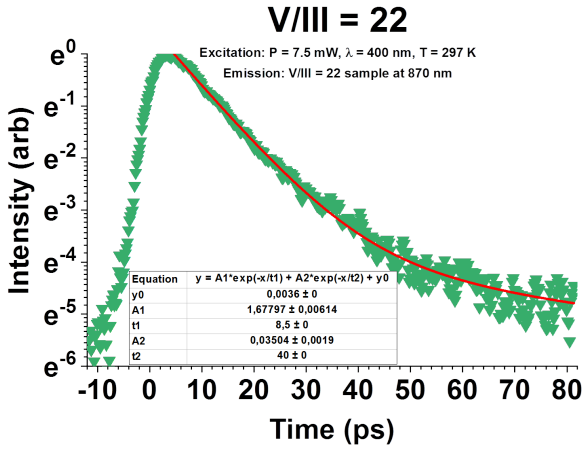

Figure 3.3: Excitation $\lambda = 400\,\text{nm}$, P = 7.5 mW, T = 297 K. V/III = 22 was a growth parameter studied further in this thesis. All of the NW samples measured at this time exhibited a biexponential decay but the V/III = 22 sample is shown as an example. One different time scales it has at least two mechanisms quenching radiative recombination. It follows a trend similar to $I = 1.7e^{\frac{-t}{8.5}} + 0.035e^{\frac{-t}{40}} + .0036$. The first and second order decay constants are 8.5 ps and 40 ps respectively.

electrons and holes from recombining radiatively. That being said, it is not trivial to determine if these particular NWs would behave differently (or show the same trends) with their surfaces passivated. Perhaps growth conditions primarily influence the volume of the nanowire. If so, the defining difference between these arrays might not be revealed until surface effects are mitigated to such an extent that voluminal characteristics can be observed. This is why passivation was attempted.

3.2 Plasma

Time-resolved photoluminescence spectroscopy was used to investigate the opto-electronic properties of gallium arsenide nanowires subjected to a nitrogen plasma (see Section 2.1.5. It has been shown in the literature that bulk GaAs can be passivated by plasma nitridation. However, very little (if any) research has shown the ability of nitrogen plasma to passivate the surfaces of GaAs NWs. Since nanowire properties often deviate significantly from their thin film and bulk counterparts, it was not at all clear if such a process could be emulated on NW arrays.

H_2/N_2 Plasma Time	L ($\pm 0.1\,\mu$m)	D (± 5 nm)	V/III Ratio	Sample
3s/10s	1.1	160	105	10669
3s/20s	1.1	160	105	10669
3s/40s	1.1	160	105	10669
12s/10s	1.8	160	66	10673
12s/20s	1.8	160	66	10673
12s/40s	2.4	160	66	10672[2]

Table 3.2: Properties of the nanowire samples measured. Due to equipment and laboratory changes, new NW arrays could not be grown at this time and therefore older, various NWs were repurposed. [2]Grown without HBr.

The process developed by Losurdo et al. and described in Section 2.1.5 was chosen as a starting point. Due to the uncertainty of the process, even concerning basic questions like "Will nitrogen incorporate into the NWs?", a diagnostic tool was needed to provide feedback. Because TRPL was available and had effectively been used to measure radiative recombination in the V/III ratio NW samples, it was decided that continuing with this setup offered several advantages over alternative methods. XPS, for example, could have taken as long as several months to get results. It would have been hard to justify using the time and resources for such an uncertain process. Similarly, using TEM would have been unnecessary and too large a deviation from the theme of this thesis. So, TRPL was chosen. Table 3.2 lists the properties of the samples characterized by this experiment.[1]

As described in the Sections 2.1.3 and 2.1.5, all samples were treated with HCl prior to plasma nitridation. This was to remove oxides and surface contaminants and increase the likelihood that radicals would interact with the crystal surface. After preparation, samples were illuminated with the setup described in Section 2.1.1 at power, P = 6.0 mW, wavelength = 400 nm, T = 297 K. Emission was averaged over 100 exposures collected at 1 s per exposures. Emission slices have been averaged across the peak intensity region near the GaAs bandgap (871 nm). Figure 3.4 shows the emission from six samples subjected to H_2 and 97% N_2 - 3% H_2 remote plasmas.

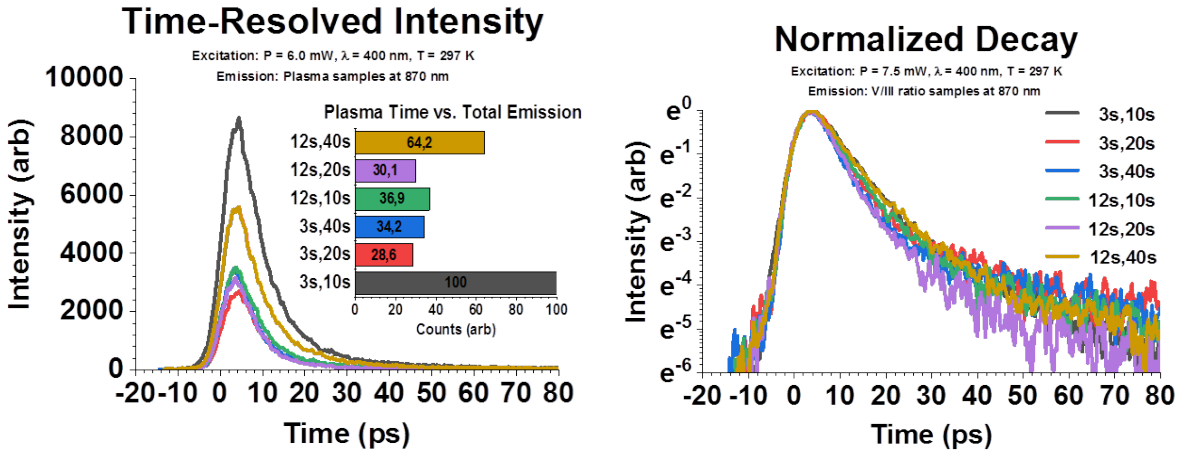

(a) (b)

Figure 3.4: Time-dependent photoemission intensity of nanowires treated with different plasma conditions. Excitation power = 6.0 mW, wavelength = 400 nm, temperature = 297 K. The #,# label denotes the length of H_2 and N_2 plasma times respectively. a) Time-resolved intensity curves at peak emission, 0 s represents the time of half-peak intensity b) Normalized intensity curves showing relative decay rates across samples.

Again, discerning a unifying pattern between plasma time and photoluminescence signal was difficult. See Figure 3.4. Consider, for example, the pattern-defying sample treated with a 12s/40s H_2/N_2 plasma. Its intensity and lifetime characteristics seem to break what could otherwise be speculated: that 3s/10s is sufficient to clear the NW surface and subsequently convert it to GaN, and that any time spent subjected to plasma beyond that is unnecessary and results in damage to the NWs. This was a trend observed in published literature, but the 12s/40s sample defies it. Another possibility considered was that the samples' differences were simple uninformative, that they might be a consequence

[1]Due to laboratory changes preventing growth of new nanowires, old samples (two years in ambient cleanroom environment) had to be measured, limiting comparison.

of unknown, unintentional or random differences. However, this cannot be known. The measurements were trusted and like with the previous measurements, a subset of the samples was more closely examined for an intelligible pattern. The 3s/10s, 3s/20s and 3s/40s samples were chosen because they were cleaved from the exact same larger piece, and because there was only one variable among them, N_2 plasma time. See Figure 3.5.

Looking in more detail at Figure 3.5a, the 3.5x larger intensity of the 3s/10s sample is stark. The 3s/20s and 3s/40s samples looked quite similar however. So, in conjunction with the increased lifetime observed in Figure 3.5b, these were taken as evidence for the pattern observed by Losurdo et al shown in Figure 1.4b. Namely, that short plasma times create thinner layers of GaN, cause less damage to the crystal and reduce non-radiative recombination. Also observed, (discussed further in Section 3.5) was that the 3s/10s sample appears to have a straighter (ln(y) scale), more single-exponential decay than the other samples.

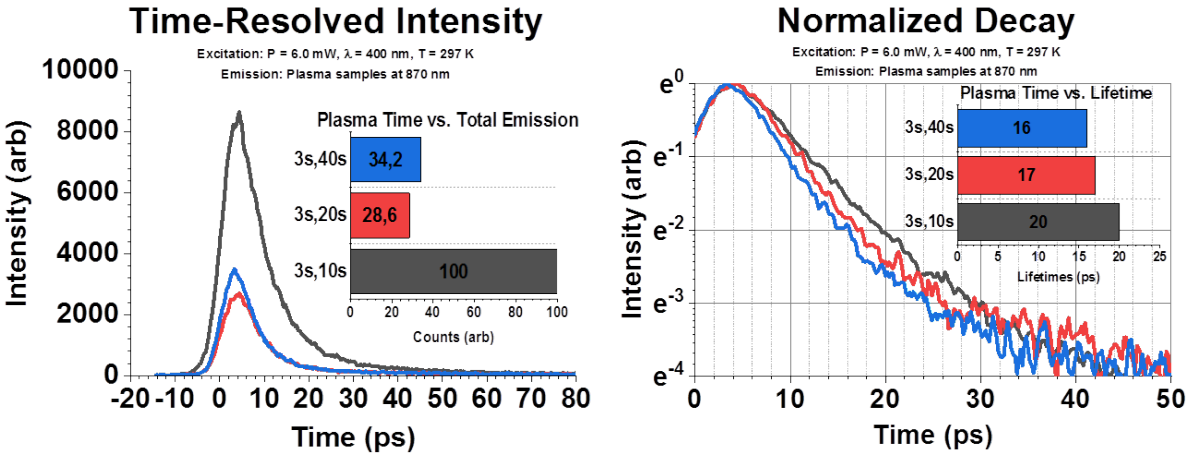

(a) (b)

Figure 3.5: Time-dependent photoemission intensity of identical nanowire samples treated with different plasma conditions. Excitation power = 6.0 mW, wavelength = 400 nm, temperature = 297 K. a) Time-resolved emission curves showing a factor of 4 increase the NWs exposed to 3s/10s plasmas b) Normalized intensity curves showing relative photoluminescence lifetime across identically grown samples.

Lastly, Figure 3.6 gives a closer look at the decay dynamics of the 3s/10s sample. It is biexponential, which indicates that at least two mechanisms (possibly states) contribute to the reduction of radiative recombination. One is on the time scale of single picoseconds and the other on the order of tens of picoseconds. The first and second order decay constants are 7 ps and 38 ps respectively.[2] Because these were the best values observed in these samples, it was the treatment procedure selected for further measurements.

Overall, the most notable observation was a lack of evidence for passivation. As explained in Section 1.2.2, the evidence for GaN-based passivation is strong, and despite several attempts to convert the surface of the nanowires to GaN using plasma, no order of magnitude changes in photoluminescence were observed. It is known that radiative lifetime, for example, has the potential to be on the order of nanoseconds. To learn more about why it was not, more measurements were planned.

[2]It might be noted here that these constants resemble those of Figure 3.3, but the samples should not be strongly compared because the nanowires were grown at different times and under different conditions.

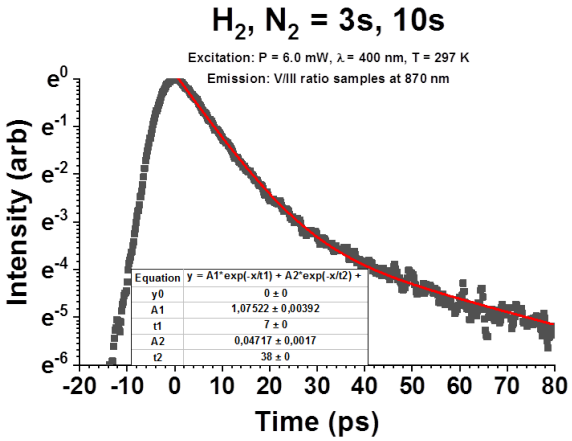

Figure 3.6: Excitation power = 6.0 mW, wavelength = 400 nm, temperature = 297 K. H_2 time = 3 s, N_2 time = 10 s was the plasma parameter studied further in this thesis. Though all of the NW samples measured at this time exhibited a biexponential decay, the 3s/10s sample less so. This was considered as evidence of removing some non-radiating midgap states. It is shown as an example and for future reference. The best curve fit obtained was $I = 1.08e^{\frac{-t}{7}} + 0.047e^{\frac{-t}{38}}$. The first and second order decay constants are 7 ps and 38 ps respectively.

3.3 Hydrazine on Plasma

Having not observed any strong passivating effects from the plasma treatments, and only observing very short lifetimes near the streak camera's limit, the hydrazine-sulfide solution developed by Berkovits et al. seemed like the most appropriate passivation method to explore for continuation. This is primarily because it had been well documented in literature and two soon-to-be published experiments reporting on its effectiveness for GaAs NWs were known about. Due to laboratory changes new NWs could not be grown. It was therefore decided that using hydrazine on the samples previously treated by N_2 plasma would provide the two-fold benefit of demonstrating the hydrazine process and/or expanding what was already known about the plasma samples. If, for example, the NWs would exhibit signs of passivation, it could be concluded that the plasma had not previously converted the surface. If no changes were observed, it could be speculated that the plasma treatment procedure resulted in a surface layer which prevented a reaction with hydrazine. This is so because the hydrazine solution functions such that only As and O are selectively removed from the surface and the nitridation itself occurs only at the top monolayer. Thus, for example, if the plasma treatments resulted in the creation of GaN with a high concentration of defects, the hydrazine solution could have no influence.

After preparation, samples were illuminated with the setup described in Section 2.1.1 at power, P = 3.4 mW, wavelength = 400 nm, T = 297 K. Emission was averaged over 200 exposures collected at 1 s per exposures. Emission slices were averaged across the peak intensity region at the GaAs bandgap (871 nm). Though the same six samples were measured, a similarly reduced data set will be shown for clarity. See Figure 3.7. The first observation made (Figure 3.7a) was that relative intensities had shifted. Unlike previously, here the 3s/40s sample emitted the most. The overall signal strength was quite low however (80% decrease) and disparities are by less than a factor of two. This reduction and convergence of values was observed in the decays as well. Shown in Figure 3.7b, the most surprising result was that radiative decay lifetime actually decreased after using hydrazine. Unlike the passivation effect observed by Berkovits et al. (large increase in intensity and reduction of surface states) the measurements after treatment with hydrazine

showed only worsened optoelectric properties.

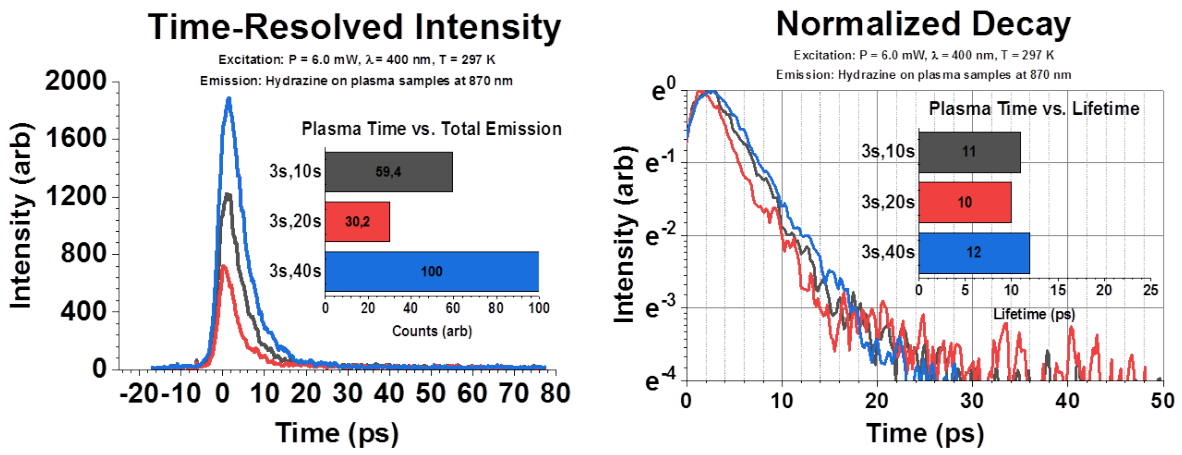

(a) (b)

Figure 3.7: Time-dependent photoemission intensity of identical nanowire samples treated with different plasma conditions, and then treated with identical hydrazine solutions. Excitation power = 6.0 mW, wavelength = 400 nm, temperature = 297 K. a) Time-resolved emission curves showing a factor of 4 increase in the emission intensity from the NWs exposed to 3s/10s plasmas before hydrazine b) Normalized intensity curves showing relative photoluminescence lifetime across identically grown samples.

Speculations were made as to the cause of this observation. The hydrazine procedure used contained no known discrepancies; the intention was to use an identical process. The details of how hydrazine would interact with a nanowire surface that had been subjected to a plasma is unknown and out of the scope of this project. However, due to known chemistry, it seemed reasonable to conclude that the solution would either have no significant effect or it would create a GaN surface from a non-GaN surface. Because an apparent reverse-passivation effect was observed two possibilities were considered. Either the hydrazine solution was ineffective for passivation (indeed counter-productive), or the solution did not interact with the nanowires at all, and some other factor degraded their optoelectronic quality. Alternatively, it could be doubted whether the observed measurements were actually probing the intentional changes made to the nanowires. Perhaps the measurement differences were the result of some other unknown, unintentional or random changes in the samples.

It was at this point that another factor had to be considered. Since the previous measurements had been made, equipment failure caused the setup to be unusable for an extended period of time. It was thus suspected that in the meanwhile, the long exposure of the samples to ambient air could have degraded their quality. If they developed a thick oxide for example, it seemed possible the hydrazine solution never came in contact with the GaAs nanowires themselves. This speculation gained support after the next measurements were conducted (Section 3.4).

Because of the seemingly large unknowns associated with the old and plasma treatment samples, it was decided that until new nanowires could be grown, it could be beneficial to reexamine the better known V/III ratio samples. They offered the benefits of: being more recently grown, being grown under similar conditions, and having prior TRPL measurements done on them. Accordingly, another experiment was done.

3.4 Hydrazine

In order to evaluate the effect of hydrazine on the nanowires, it was decided that the previously measured V/III ratio samples should be cleaved to create references. Accordingly, two sets of samples were prepared and measured. After cleaving, each V/III ratio sample generated a reference sample and a sample to be treated with hydrazine. In this way, the procedure used by Berkovits et al. could be verified and at the same time, the identical NW samples could be directly compared (HCl to hydrazine). So, half of the samples underwent the standard HCl deoxidation procedure and half of the samples were put in the hydrazine-sulfide solution. The processes are described in Section 2.1.

After preparation, samples were illuminated with the setup described in Section 2.1.1 at power, P = 3.4 mW, wavelength = 400 nm, T = 297 K. Emission was averaged over 200 exposures collected at 1 s per exposures. Emission slices were averaged across the peak intensity region at the GaAs bandgap (871 nm).

3.4.1 V-III Ratio

When the same V/III ratio samples were again deoxidized with HCl and measured after a long wait (several weeks), the results obtained followed the pattern observed in Section 3.1. That is, as V/III ratio decreased, photoluminescence lifetime increased. Consider Figure 3.8b. This time however, the photoluminescence intensity of the V/III ratio = 22 sample was the highest, by an order of magnitude.

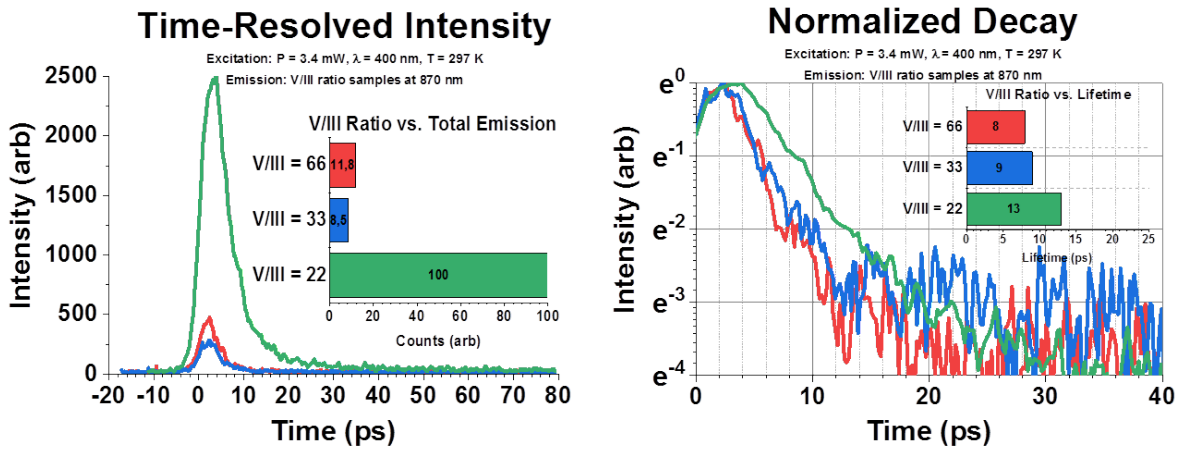

(a) (b)

Figure 3.8: Time-dependent photoemission intensity of HCl-treated nanowires grown with different V/III ratios. Excitation power = 3.4 mW, wavelength = 400 nm, temperature = 297 K. a) Time-resolved intenisty curves and their total integrated intensities, showing an order of magnitude larger emission in the NWs grown at V/III ratio = 22 relative to the other samples. b) Normalized intensity curves showing relative photoluminescence lifetime across the samples. The previously observed trend of lifetimes increasing with decreasing V/III ratio was measured here as well.

3.4.2 Hydrazine

With the application of hydrazine to the V/III ratio samples came the first highly unexpected result of the project. As can be seen in Figure 3.9 neither net photoluminescence

nor decay lifetime increased dramatically compared to the samples only deoxidized (Figure 3.8).

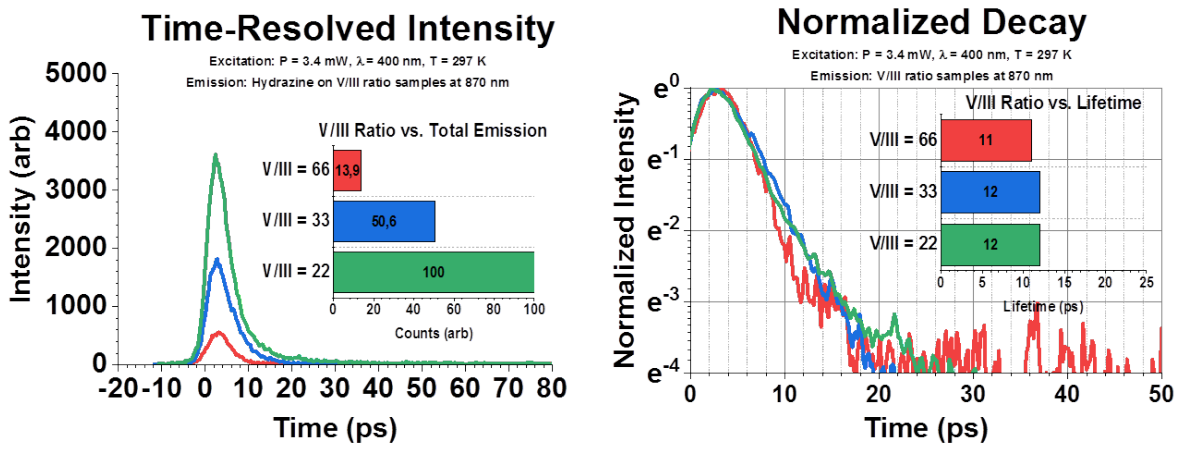

(a) (b)

Figure 3.9: Time-dependent photoemission intensity of nanowires grown with different V/III ratios and treated with a hydrazine-sulfide solution. Excitation power = 3.4 mW, wavelength = 400 nm, temperature = 297 K a) Time-resolved intensity curves show an order of magnitude larger intensity from the NWs grown at V/III ratio = 22 relative to the standard ratio V/III = 66. b) Normalized intensity curves showing convergence of photoluminescence lifetimes among the samples.

3.5 Passivation Matrix: Low Temperature Characterization

At this point a significant reevaluation was done and several things were considered. First, a sample of P3OOT (high HOMO level conjugated polymer described in Section 1.2.3) had arrived and its passivating effect had yet to be characterized. Second, the lack of any stark passivating effects from the well-established hydrazine method had not been observed. Third, no strong passivation of any kind had been observed. This lead to serious doubts about the meaningfulness of interpreting relatively minor changes in sample emission. Indeed, even room temperature measurements of these GaAs nanowires entirely. If photoluminescence intensity and lifetime can change by orders of magnitude, it was not clear how meaningful changes on the order of ∼1 ps or ∼5x intensity were. Lastly, one of the primary goals for this thesis was to systematically try and compare several passivation methods with the ultimate goal of finding a useful method for commercial production and/or academic research. Accordingly, the structure of the final experiment took shape, with the incorporation of two new ideas.

The structure of this experiment was a full matrix comparing: nanowires unaltered from the condition the were grown in (as-grown), deoxidized nanowires using the HCl method, nanowires treated with hydrazine, nanowires subjected to a nitrogen plasma, and nanowires coated in conjugated polymer with a high HOMO level. These five samples were thought to give a good and comprehensive overview of how the university's nanowires luminesce and what treatments (if any) influence them. Two changes were made with the hope of provoking order of magnitude differences between samples. The first was temperature. In numerous publications, including two that inspired this thesis,

the authors conducted low temperature PL measurements. It was tacitly acknowledged but often undiscussed in literature that PL increased with decreasing temperature. Indeed, this was observed at Lund University as well. Due to the increased complexity of the measurement setup (eg. liquid nitrogen, cryostatic sample chamber etc.) it was not utilized initially. The second change adopted was one to nanowire growth. It was reported by Jiang et al. (and substantiated within Lund University) that high temperature annealing of nanowires (750 °C for 2 min) post growth would reshape their cross sections into hexagons with exclusively {110} facets.[81] Because surfaces have an outsized influence on nanowire functioning and passivation is largely a question of how to manage these surfaces, it seemed prudent to control and study them.

Specifically: Losurdo et al. only demonstrated the passivating influence of nitrogen plasma on GaAs(100) substrates, not NWs or {110} surfaces; Berkovits et al. published copiously about the surface-dependency of their hydrazine treatment; and Yong et al. only reported passivation with their predominately {112} faceted NWs. Accordingly, reconstructing the NW surfaces to achieve more uniformity seemed appropriate. To measure these samples and treatments it was decided that the seemingly best V/III growth ratio would be used, V/III = 22. For completeness, two reference samples were measured as well, a bare GaAs substrate and a GaAs substrate coated with a polymer film. An outline of the matrix is shown in Table 3.3 below.

Sample/Condition	**As-grown**	**HCl**	**Plasma**	**Hydrazine**	**Polymer**
Annealing/Temperature	x/100 K	x/100 K	x/100 K	x/100 K	x/100 K
Annealing/Temperature	x/300 K	x/300 K	x/300 K	x/300 K	x/300 K
Annealing/Temperature	✓/100 K	✓/100 K	✓/100 K	✓/100 K	✓/100 K
Annealing/Temperature	✓/300 K	✓/300 K	✓/300 K	✓/300 K	✓/300 K

Table 3.3: Properties of the nanowire samples measured for this experiment. Annealing at elevated temperature (750 °C) was used to reshape the NWs for surface uniformity. Temperature dependent measurements were conducted in order to see sample changes not observable at room temperature.

Due to the limited scope of this thesis, only two temperatures and one excitation intensity were selected. Liquid nitrogen was used to cool the samples which were kept in an evacuated cryostatic chamber. Equipment limitations led to the selection of two stable measuring temperatures, 100 K and 300 K. The excitation power used was P = 3.0 mW because it was the lowest power that showed a signal at 300 K and emission was expected to increase at lower temperature.

The experiment provided a large amount of data that cannot be fully discussed within this report. What follows, however, is a thorough summary of the most important observations and conclusions. Figure 3.10 below gives an overview of the different samples' intensities and lifetimes. 100 K measurements are shown on the left half in purple and pink and 300 K measurements are shown on the right half in blue and orange. The left bars (bluish) are measured on the left side with logarithmic axis due the large changes in emission intensity. The right bars (reddish) are measured on the right side with a linear axis. As described above, each sample has a high temperature annealed (HTA) counterpart. Without attempting to focus too much on the details, Figure 3.10 should give a sense of the scope of the experiment and reveal a few important general observations. The first is that temperature does in fact induce a large change in photoluminescence (left bars and left y-axis). The low temperature samples on the left half of the x-axis

emitted two to three orders of magnitude more than room temperature samples on the right half of the x-axis. This came with a smaller but noteworthy increase in photoluminescence lifetime (right bars and right y-axis). The second, is that the plasma samples are outliers. They exhibited much higher intensities and longer lifetimes than all other samples. The third, is that annealing did not result in a large or consistent difference in sample photoluminescence intensity or lifetime. These patterns are even clearer upon closer examination. Though, not every sample measurement is worth discussing. For the sake of brevity and readability, further discussion of the data will focus on a smaller and more important subset of samples. As is shown by careful examination of Figure 3.10a, annealing had no discernable influence on sample intensity or lifetime.

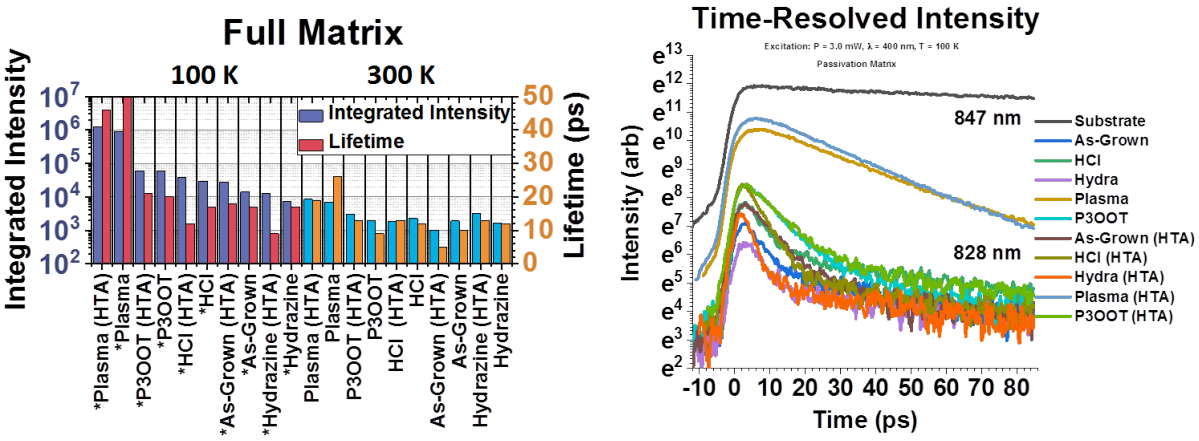

(a) (b)

Figure 3.10: a) Bar chart summarizing all NW samples. Bluish colored left-bars are measured by the logarithmic y-axis on the left. Reddish colored right-bars are measured by the linear y-axis on the right. HTA means the sample was annealed at high temperature for facet reshaping. * and their corresponding colors signify that the measurements were collected at 100 K (left-half) and 300 K (right-half). Note three things. 1) A reduction in characterization temperature induces a large change in photoluminescence intensity (left bars and left y-axis) and a smaller but notable increase in photoluminescence lifetime (right bars and right y-axis); 2) Plasma samples (independent of annealing) exhibited much higher intensities and longer lifetimes than all other samples; 3) Annealing (HTA) did not result in a large or consistent observed difference in sample photoluminescence intensity or lifetime. b) Time-dependent photoemission intensity of nanowire samples at 100 K and a GaAs substrate for reference. The same observations shown by the data in Figure a) can be seen here. Note how the emission of the non-nanostructured, unpassivated substrate is completely unlike (and superior to) that of NWs. This is a consequence of surface-to-volume ratio and is why passivation is so important.

3.5.1 300K

The 300 K data shown in Figure 3.11 is quite noisy and difficult to interpret even with just the reduced set of data shown in Figure 3.11b. The following however should be noted. First, regardless annealing conditions, the plasma treated samples clearly exhibit stronger and longer photoluminescent emission than the other samples. Relative to the as-grown nanowire sample, intensity increased by almost an order of magnitude. Clearly, more charges were recombining radiatively and over a longer time span. Second, as-grown and HCl-treated samples emitted most poorly, with the as-grown sample's decay not even being resolvable by the setup. Third, though difficult to say definitively, the polymer and hydrazine treated samples appear to be about the same. Intensity and lifetime were

somewhat improved. Sample lifetimes were imprecisely estimated as follows: plasma = 19 ps, P3OOT = 13 ps, hydrazine = 13 ps, HCl = 13 ps, as-grown = 5 ps. 5 ps approaches the instrument response limit of the setup and due to the small signal-to-noise ratio, all of the values should be thought of qualitatively. Furthermore, if the as-grown emission really is decaying faster than the instrument can resolve, this can be thought of as an indicator of passivation, because all of the other samples' emission decays are clearly resolvable. In this sense, we can think of all of the passivation treatments as capable of "turning on" the nanowires. All of the treated samples, though especially the NWs subjected to plasma, exhibited a significant increase in intensity and a radiative decay that became resolvable by the streak camera.

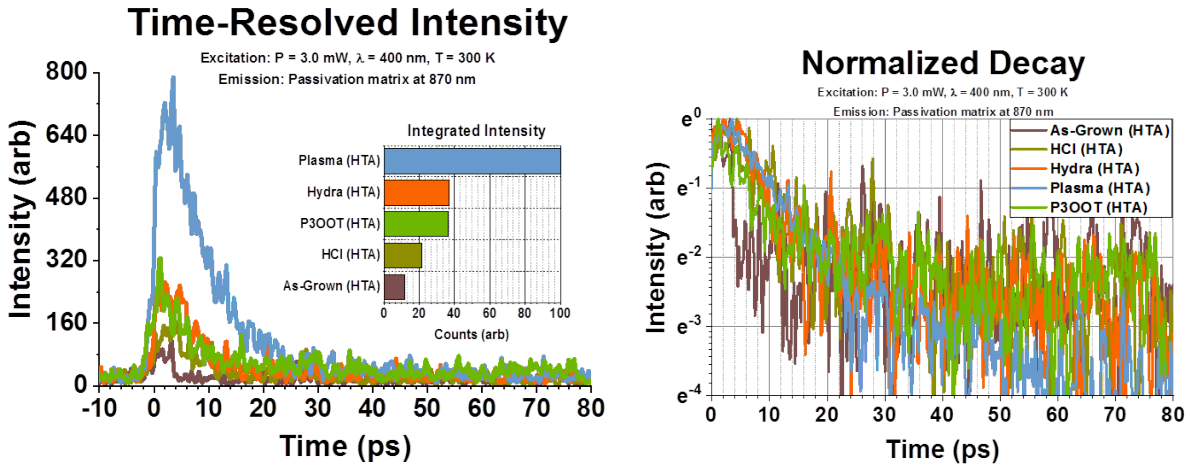

(a) (b)

Figure 3.11: Time-dependent photoemission intensity of NWs passivated by different methods. Though signal-to-noise is very low, it is still clear that the plasma treatment improved the NWs photoluminescence significantly relative to the other samples. Quantitative measurements are difficult to make but qualitatively there is a significant improvement in both photoluminescence intensity and lifetime.

A noteworthy feature of the data observed was the ability to discriminate between substrate and NW emission. This was observed at both 300 K and 100 K as shown in Figures 3.12a and b respectively. The distinct substrate emission peak is due to the fact that it is highly p-doped with zinc. This observed band-acceptor radiative recombination peak was located at 891 nm, very close to the 892 nm value predicted empirically in literature.[94] Also note the blue-shift at lower temperature. Both intrinsic NW emission peaks 871 nm at 300 K and 828 nm at 100 K are identical to the temperature dependent bandgap of GaAs characterized by the Varshni equation with up-to-date parameters.[95, 96]

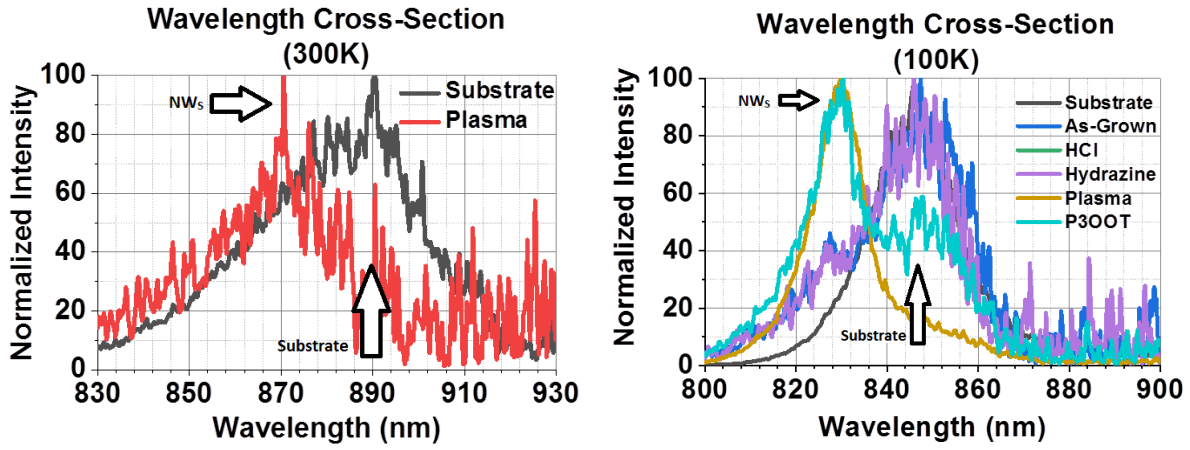

(a) (b)

Figure 3.12: Wavelength cross-sections at peak intensity. Intrinsic NWs' emission can be distinguished from substrate emission (which is highly p-doped) due to its higher energy and shorter wavelength. a) Due to weak emission of the other NW samples, only the plasma sample is compared with the substrate. NWs = 871 nm, substrate = 891 nm b) Note that the plasma sample is the only sample in which the NW emission dominates the substrate emission. NWs = 828 nm, substrate = 847 nm.

3.5.2 100K

The data at 100 K is much clearer however. Despite identical excitation and collection parameters, the emission is entirely different. This is shown in Figure 3.10, but a closer examination of the emission in Figures 3.13a and b shows just how dramatic the shift is. Figure 3.13a, for example, shows a more than twenty-fold increase in photoluminescence intensity. Figure 3.13b shows a more than doubling of lifetime. Interestingly, the hydrazine treated sample had both the lowest photoluminescence intensity and the shortest lifetime, significantly worse than the as-grown nanowires. This repeated depassivating effect observed from the solution is still unclear and in contrast to existing literature. Careful precaution was taken to follow a procedure identical to that published by Berkovits et al., yet on several occasions the measurements collected for this project failed to record a similar trend.

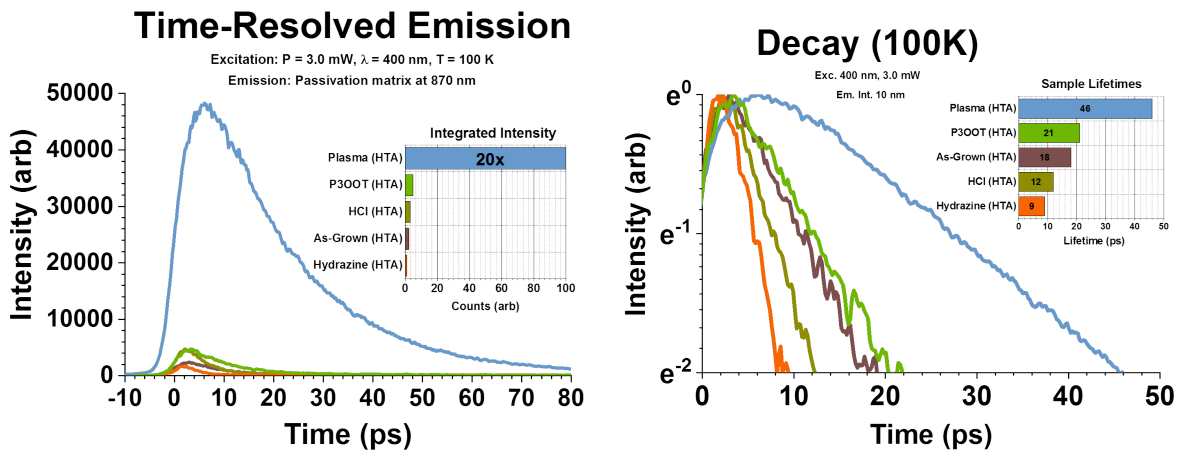

(a) (b)

Figure 3.13: Time-resolved emission at T = 100 K of annealed nanowire samples passivated by different methods 870 nm. a) The integrated emission intensity of the plasma sample is more than twenty times greater than that of the nanowires passivated by polymer and one hundred times that of hydrazine. b) The photoluminescence lifetimes of the samples vary significantly. The plasma sample's lifetime more than doubles that of the as-grown and polymer coated samples and is a 5x longer than hydrazine.

One way to explain the large influence of the plasma treatment on the nanowires is by considering the band diagram shown in Figure 1.2. The commonly accepted explanation for the observed poor optoelectronic quality of GaAs surfaces is due to excess arsenic.[24, 58, 59] Surface arsenic that oxidizes, segregates, or exists in antisites can create midgap electronic states. The nitrogen plasma treatment, with its combined wet and H_2 plasma pre-etches appear to have eliminated one or more of these midgap states. With these states removed, excited electrons and holes have many, many fewer sites to relax without recombining radiatively. One interesting thing to note however is that this was a strongly temperature dependent phenomenon. At 300 K the improvement of plasma treated nanowires over the other samples was significantly smaller. This temperature dependence of the midgap states suggests a process that is thermally activated. Unfortunately, it is out of the scope of this thesis to do additional temperature-dependent measurements. However, this seems like an idea well worth exploring.

Chapter 4

Conclusion and Outlook

4.1 Conclusion

Several key findings of the research done for this thesis are summarized, starting with the most surprising. The biggest mystery observed throughout these experiments was the lack of any apparent passivation effect due to hydrazine. This could perhaps have been expected the first time when it was used post-plasma, because the NW surfaces may already have been converted to GaN. However, the two subsequent uses of hydrazine and their associated lack of passivation are to this point inexplicable. In yet-to-be published experiments of GaAs NWs that report hydrazine's passivating effects, each contain one procedural difference compared to the process used in this thesis. One involved a pre-treatment of the NWs and one modified the solution relative to the procedure published by Berkovits et al. The treatment used in this thesis however, replicated the process published exactly. Speculation will continue as to why no passivation was observed, but until a satisfactory explanation can be obtained, because of the safety risks associated with hydrazine chemistry, continued use for NW passivation cannot be recommended.

Another two important general points about the method used in this thesis should be noted. To date, all the NWs characterized with TRPL at room temperature yielded very low emission intensity and very fast decay. Decays were slow enough to be resolved by the streak camera, but not by much. Furthermore, emission intensity was weak enough such that finding and accurately measuring it was an additional challenge, often requiring excitation power near the laser's maximum. It is suspected that very high excitation can introduce unique problems like damage to the sample and irreproducibility in measurement. Thus, there is a double bind. Poor photoluminescence of the NWs makes measurement difficult and requires using the TRPL setup near the limit of its capabilities, but using the setup near its limits reduces its ability to characterize the samples. Alternatively, complicating the experimental setup further by doing low temperature measurements introduces a new problem. At low temperatures, characterization of poorly emitting samples becomes much more accurate and detailed, but at the expense of needing to spend significant time and effort just to characterize a material's poor characteristics. This is probably not worth a researcher's time.

Accordingly, future use of this TRPL setup to characterize weakly emitting samples should be done only after careful consideration. Faster and simpler methods like SSPL could be considered. If TRPL is to be used, now that a starting point for GaAs NW passivation has been identified (plasma nitridation), perhaps single, brief measurements can be made without full characterization. For example, a 3s,10s plasma sample could

be kept as a reference, and under standardized excitation and collection parameters new treatments could be quickly compared. Full analysis would proceed only if improvements were observed. This would require a characterization of the plasma treated sample's degradation over time, but that is probably a useful endeavor in and of itself. Literature suggests a relatively stable and robust surface due to the strength of GaN bonding.

The second general point to be made about these measurements is that if NWs are to be used for photovoltaics, they are almost certainly going to be used at temperatures around 300 K (or higher). Accordingly, if the 300 K PL of the NWs directly correlates with photovoltaic performance, it is probable that none of the samples measured for this thesis are sufficiently passivated. In other words, these room temperature TRPL measurements may indeed be accurately characterizing the samples, but the magnitude of differences observed might be irrelevant to photovoltaics. That is a question that has yet to be answered and is out of the scope of this thesis. Still, the low temperature data gives valuable input on the effect of passivation, and can be used to motivate and understand further studies.

Finally, the most promising result of these experiments is that plasma nitridation can be used to achieve a passivating effect in GaAs NWs. This may actually be the first public evidence demonstrating the treatment's effectiveness on GaAs nanowires, not just substrates. Unfortunately, a comprehensive characterization of this passivation is out of the scope of this thesis. For example, no TEM or XPS measurements have been done and it is hitherto unknown whether it is the internal or surface properties of the NWs that limits their photoluminescence. Regardless, after plasma treatment the NWs underwent a dramatic change. This change was visible at 300 K but was clearest at 100 K. Relative to all other samples and treatments, the nanowire arrays that received a plasma treatment seem to have had their surface improved in such a way that when electrons and holes were generated, many, many more were able to recombine radiatively across the bandgap. Radiative recombination in the plasma treated NWs was 100x greater than in the NWs treated by hydrazine and 50x greater than in the samples simply left as they were grown. The explanation for this is that the plasma process removed midgap states that allowed electrons and holes to combine without photoemission. As reported in literature, the removed states are probably related to excess arsenic that can lead to defects and oxides. The plasma procedure used in this thesis likely removed (and prevented reaccumulation of) a significant amount of arsenic at the NW surface by one or more of the following three processes: 1) wet etching, 2) H_2 remote plasma, and 3) 97% N_2 - 3% H_2 remote plasma. With this removed, the bandgap at the surface was partially restored and more band edge recombination occurred. Despite the success of this method however, several things have been identified as opportunities for potential improvement in the future. They are listed below.

4.2 Suggestions for Improvement

4.2.1 HCl

Regarding the HCl deoxidation procedure, it has been observed that HCl solutions in water evaporate from the sample surface quite slowly, even with the assistance of N_2 flow. During the literature review conducted for this thesis it was noted that several other deoxidation by HCl procedures exist. One apparently successful method used HCl in isopropanol.[97, 98] If future procedures cannot be done in a glove box, isopropanol,

which evaporates more quickly, could be used to dilute HCl and expose the GaAs to less time in oxygen.

4.2.2 Polymer

The sample of P3OOT used in this thesis was obtained quite late in the process. Accordingly, much is still unknown. Future study of the polymer should involve characterizing its absorbance and emission spectra and getting a better estimate about its HOMO level. Furthermore, the quality of its thin films was only briefly explored due to time limitations and for a more comprehensive study of its effectiveness, a well characterized procedure should be developed (eg. embedding vs. thin films, optimized concentrations, deposition method etc.). The process and information detailed in this thesis should offer a good starting point for anyone interested. If access to a functioning glove box with hotplates is limited, the HCl treatment recommended above could become important as well. On a final note, a thorough comparison with Yong et al. may be difficult because their NWs were wurtzite, enclosed by {112} facets and measured at 77 K.

4.2.3 Plasma

Unfortunately, due to equipment problems, only one comparison of plasma conditions was conducted, at room temperature. Accordingly, the recommended process may still not yet be fully optimized. Since this was the most successful method employed, it is recommended that future studies optimize this process before continuing.

For those interested in charge carrier dynamics and radiative recombination, a logical next step would be to fully characterize the NW photoluminescence. A full temperature and power dependent characterization could be done. If combined with XPS and ellipsometric measurements, a very thorough understanding could be developed.

Bibliography

[1] C. B. Field, V. R. Barros, D. J. Dokken, K. J. Mach, M. D. Mastrandrea, T. E. Bilir, M. Chatterjee, K. L. Ebi, Y. O. Estrada, R. C. Genova, B. Girma, E. S. Kissel, A. N. Levy, S. MacCracken, P. R. Mastrandrea, and L. L. White, *IPCC, 2014: Summary for policymakers. In: Climate Change 2014: Impacts, Adaptation, and Vulnerability. Part A: Global and Sectoral Aspects. Contribution of Working Group II to the Fifth Assessment Report of the Intergovernmental Panel on Climate Change*. Cambridge, United Kingdom and New York, NY, USA: Cambridge University Press, 2014.

[2] I. McDougall, F. H. Brown, and J. G. Fleagle, "Stratigraphic placement and age of modern humans from kibish, ethiopia," *Nature*, vol. 433, p. 733, 2005.

[3] R. Pachauri and L. Meyer, *IPCC, 2014: Climate Change 2014: Synthesis Report. Contribution of Working Groups I, II and III to the Fifth Assessment Report of the Intergovernmental Panel on Climate Change*. Geneva, Switzerland: IPCC, 2014.

[4] M. D. Shear, "Trump will withdraw u.s. from paris climate agreement," *New York Times*, June 1, 2017. https://www.nytimes.com/2017/06/01/climate/trump-paris-climate-agreement.html.

[5] G. Otnes and M. T. Borgström, "Towards high efficiency nanowire solar cells," *Nano Today*, vol. 12, pp. 31–45, 2017.

[6] M. A. Green, "Commercial progress and challenges for photovoltaics," *Nature Energy*, vol. 1, no. 1, 2016.

[7] J. Wallentin, N. Anttu, D. Asoli, M. Huffman, I. Åberg, M. H. Magnusson, G. Siefer, P. Fuss-Kailuweit, F. Dimroth, B. Witzigmann, H. Q. Xu, L. Samuelson, K. Deppert, and M. T. Borgström, "Achieving 13.8% efficiency by exceeding the ray optics limit," *Science*, vol. 339, no. 6123, pp. 1057–1060, 2013.

[8] P. Krogstrup, H. I. Jørgensen, M. Heiss, O. Demichel, J. V. Holm, M. Aagesen, J. Nygard, and A. Fontcuberta i Morral, "Single-nanowire solar cells beyond the shockley–queisser limit," *Nature Photonics*, vol. 7, no. 4, pp. 306–310, 2013.

[9] I. Aberg, G. Vescovi, D. Asoli, U. Naseem, J. P. Gilboy, C. Sundvall, A. Dahlgren, K. E. Svensson, N. Anttu, M. T. Bjork, and L. Samuelson, "A gaas nanowire array solar cell with 15.3% efficiency at 1 sun," *IEEE Journal of Photovoltaics*, vol. 6, no. 1, pp. 185–190, 2016.

[10] K. Deppert, J.-O. Bovin, J.-O. Malm, and L. Samuelson, "A new method to fabricate size-selected compound semiconductor nanocrystals: aerotaxy," *Journal of Crystal Growth*, vol. 169, no. 1, pp. 13–19, 1996.

[11] P. A. Alekseev, M. S. Dunaevskiy, V. P. Ulin, T. V. Lvova, D. O. Filatov, A. V. Nezhdanov, A. I. Mashin, and V. L. Berkovits, "Nitride surface passivation of gaas nanowires: impact on surface state density," *Nano Letters*, vol. 15, no. 1, pp. 63–8, 2015.

[12] M. Yao, N. Huang, S. Cong, C. Y. Chi, M. A. Seyedi, Y. T. Lin, Y. Cao, M. L. Povinelli, P. D. Dapkus, and C. Zhou, "Gaas nanowire array solar cells with axial p-i-n junctions," *Nano Lett*, vol. 14, no. 6, pp. 3293–303, 2014.

[13] H. J. Joyce, P. Parkinson, N. Jiang, C. J. Docherty, Q. Gao, H. H. Tan, C. Jagadish, L. M. Herz, and M. B. Johnston, "Electron mobilities approaching bulk limits in "surface-free" gaas nanowires," *Nano Letters*, vol. 14, no. 10, pp. 5989–5994, 2014.

[14] H. J. Joyce, Q. Gao, H. H. Tan, C. Jagadish, Y. Kim, J. Zou, L. M. Smith, H. E. Jackson, J. M. Yarrison-Rice, P. Parkinson, and M. B. Johnston, "Iii–v semiconductor nanowires for optoelectronic device applications," *Progress in Quantum Electronics*, vol. 35, no. 2-3, pp. 23–75, 2011.

[15] H. Tanemura, K. Kanazawa, and H. Ikoma, "GaN-passivation of GaAs with less plasma damages: Effects of input plasma power, substrate heating and post-thermal annealing," *Japanese Journal of Applied Physics*, vol. 39, no. 4A, p. 1629–1634, 2000.

[16] C. C. Chang, C. Y. Chi, M. Yao, N. Huang, C. C. Chen, J. Theiss, A. W. Bushmaker, S. Lalumondiere, T. W. Yeh, M. L. Povinelli, C. Zhou, P. D. Dapkus, and S. B. Cronin, "Electrical and optical characterization of surface passivation in gaas nanowires," *Nano Letters*, vol. 12, no. 9, pp. 4484–4489, 2012.

[17] M. Dhankhar, O. P. Singh, and V. N. Singh, "Physical principles of losses in thin film solar cells and efficiency enhancement methods," *Renewable and Sustainable Energy Reviews*, vol. 40, pp. 214–223, 2014.

[18] P. Parkinson, H. J. Joyce, Q. Gao, H. H. Tan, X. Zhang, J. Zou, C. Jagadish, L. M. Herz, , and M. B. Johnston, "Carrier lifetime and mobility enhancement in nearly defect-free core-shell nanowires measured using time-resolved terahertz spectroscopy," *Nano Letters*, vol. 9, no. 9, pp. 3349–3353, 2009.

[19] R. R. LaPierre, A. C. E. Chia, S. J. Gibson, C. M. Haapamaki, J. Boulanger, R. Yee, P. Kuyanov, J. Zhang, N. Tajik, N. Jewell, and K. M. A. Rahman, "Iii-v nanowire photovoltaics: Review of design for high efficiency," *Physica Status Solidi RRL*, vol. 7, no. 10, pp. 815–830, 2013.

[20] V. Dagyte, E. Barrigon, W. Zhang, X. Zeng, M. Heurlin, G. Otnes, N. Anttu, and M. T. Borgstrom, "Time-resolved photoluminescence characterization of gaas nanowire arrays on native substrate," *Nanotechnology*, vol. 28, no. 50, p. 505706, 2017.

[21] K. Deppert, J.-O. Bovin, J.-O. Malm, and L. Samuelson, "A new method to fabricate size-selected compound semiconductor nanocrystals: aerotaxy," *Journal of Crystal Growth*, vol. 169, no. 1, pp. 13–19, 1996.

[22] K. Deppert, J.-O. Bovin, J.-O. Malm, and L. Samuelson, "A new method to fabricate size-selected compound semiconductor nanocrystals: aerotaxy," *Journal of Crystal Growth*, vol. 169, no. 1, pp. 13–19, 1996.

[23] R. R. LaPierre, "Numerical model of current-voltage characteristics and efficiency of gaas nanowire solar cells," *Journal of Applied Physics*, vol. 109, no. 3, pp. 1–9, 2011.

[24] C. K. Yong, K. Noori, Q. Gao, H. J. Joyce, H. H. Tan, C. Jagadish, F. Giustino, M. B. Johnston, and L. M. Herz, "Strong carrier lifetime enhancement in gaas nanowires coated with semiconducting polymer," *Nano Lett*, vol. 12, no. 12, pp. 6293–301, 2012.

[25] J. I. Pankove, J. E. Berkeyheiser, S. J. Kilpatrick, and C. W. Magee, "Passivation of gaas surfaces," *Journal of Electronic Materials*, vol. 12, no. 2, pp. 359–370, 1983.

[26] R. Carin, A. Le Moël, and J. P. Duraud, "Photoemission study of nitrogen-implanted gaas surfaces," *Journal of Applied Physics*, vol. 65, no. 12, pp. 5051–5056, 1989.

[27] C. J. Sandroff, R. N. Nottenburg, J. C. Bischoff, and R. Bhat, "Dramatic enhancement in the gain of a gaas/algaas heterostructure bipolar transistor by surface chemical passivation," *Applied Physics Letters*, vol. 51, no. 1, pp. 33–35, 1987.

[28] J. Lagowski, M. Kaminska, J. M. Parsey, H. C. Gatos, and M. Lichtensteiger, "Passivation of the dominant deep level (el2) in gaas by hydrogen," *Applied Physics Letters*, vol. 41, no. 11, pp. 1078–1080, 1982.

[29] F. Capasso and G. F. Williams, "A proposed hydrogenation/nitridization passivation mechanism for gaas and other iii-v semiconductor devices, including ingaas long wavelength photodetectors," *Journal of the Electrochemical Society*, vol. 129, no. 4, pp. 821–824, 1982.

[30] M. Losurdo, P. Capezzuto, and Bruno, "Chemistry and kinetics of the gan formation by plasma nitridation of gaas: An in situ real-time ellipsometric study," *Physical Review B*, vol. 58, no. 23, pp. 878–888, 1998.

[31] S. Anantathanasarn and H. Hasegawa, "Surface passivation of gaas using an ultrathin cubic gan interface control layer," *Journal of Vacuum Science & Technology B*, vol. 19, no. 4, pp. 1589–1596, 2001.

[32] S. Anantathanasarn, S. ya Ootomo, T. Hashizume, and H. Hasegawa, "Surface passivation of gaas by ultra-thin cubic gan layer," *Applied Surface Science*, vol. 159-160, no. 4, pp. 456–461, 2000.

[33] G. Monier, L. Bideux, C. Robert-Goumet, B. Gruzza, M.Petit, J. L. Lábár, and M.Menyhárd, "Passivation of gaas(001) surface by the growth of high quality c-gan ultra-thin film using low power glow discharge nitrogen plasma source," *Surface Science*, vol. 606, no. 13-14, pp. 1093–1099, 2012.

[34] S. A. Ding, S. R. Barman, K. Horn, H. Yang, B. Yang, O. Brandt, and K. Ploog, "Valence band discontinuity at a cubic gan/gaas heterojunction measured by synchrotron-radiation photoemission spectroscopy," *Applied Physics Letters*, vol. 70, no. 18, pp. 2407–2409, 1997.

[35] I. Vurgaftman, J. R. Meyer, and L. R. Ram-Mohan, "Band parameters for iii–v compound semiconductors and their alloys," *Journal of Applied Physics*, vol. 89, no. 11, pp. 5815–5875, 2001.

[36] M. A. Demyanenko, D. G. Esaev, A. I. Toropov, N. A. Valisheva, D. V. D. Sergey A. Dvoretsky, D. V. Gulyaev, V. A. Fateev, I. V. Marchishin, D. Y. Protasov, V. N. O. Anatoly P. Savchenko, and K. Zhuravlev, *Two-dimensional Materials for Photodetector, Chapter 6: AlGaAs/GaAs Quantum Well Infrared Photodetectors*. Reading, Massachusetts": IntechOpen, 2017.

[37] K. Tomioka, Y. Kobayashi, J. Motohisa, S. Hara, and T. Fukui, "Selective-area growth of vertically aligned gaas and gaas/algaas core-shell nanowires on si(111) substrate," *Nanotechnology*, vol. 20, no. 14, pp. 1–8, 2009.

[38] R. J. Nelson and R. G. Sobers, "Interfacial recombination velocity in gaalas/gaas heterostructures," *Applied Physics Letters*, vol. 32, no. 11, pp. 1078–1080, 1978.

[39] V. Augelli, T. Ligonzo, A. Minafra, L. Schiavulli, V. Capozzi, G. Perna, M. Ambrico, and M. Losurdo, "Optical and electrical characterization of n-gaas surfaces passivated by n2–h2 plasma," *Journal of Luminescence*, vol. 102-103, pp. 519–524, 2003.

[40] M. Losurdo, P. Capezzuto, G. Bruno, G. Perna, and V. Capozzi, "N_2–h_2 remote plasma nitridation for gaas surface passivation," *Applied Physics Letters*, vol. 81, no. 1, pp. 16–18, 2002.

[41] V. L. Berkovits, V. P. Ulin, M. Losurdo, P. Capezzuto, G. Bruno, G. Perna, and V. Capozzi, "Wet chemical nitridation of gaas (100) by hydrazine solution for surface passivation," *Applied Physics Letters*, vol. 80, no. 20, pp. 3739–3741, 2002.

[42] V. L. Berkovits, T. V. L'vova, and V. P. Ulin, "Chemical nitridation of gaas(100) by hydrazine-sulfide water solutions," *Vacuum*, vol. 57, no. 2, pp. 201–207, 2000.

[43] V. L. Berkovits, V. P. Ulin, O. E. Tereshchenko, D. Paget, A. C. H. Rowe, P. Chiaradia, B. P. Doyle, and S. Nannarone, "Gaas(111)a and b surfaces in hydrazine sulfide solutions: Extreme polarity dependence of surface adsorption processes," *Physical Review B*, vol. 80, no. 23, 2009.

[44] V. L. Berkovits, L. Masson, I. V. Makarenko, and V. P. Ulin, "Structural properties of gaas surfaces nitrided in hydrazine-sulfide solutions," *Applied Surface Science*, vol. 254, no. 24, pp. 8023–8028, 2008.

[45] V. L. Berkovits, D. Paget, A. N. Karpenko, V. P. Ulin, and O. E. Tereshchenko, "Soft nitridation of gaas(100) by hydrazine sulfide solutions: Effect on surface recombination and surface barrier," *Applied Physics Letters*, vol. 90, no. 2, pp. 1–3, 2007.

[46] V. P. Ulin, O. E. Tereshchenko, P. Chiaradia, D. Paget, B. P. Doyle, A. C. H. Rowe, V. L. Berkovits, and S. Nannarone, "Chemistry of wet treatment of gaas(111)b and gaas(111)a in hydrazine-sulfide solutions," *Journal of the Electrochemical Society*, vol. 158, no. 3, pp. 127–135, 2011.

[47] V. L. Berkovits, V. P. Ulin, M. Losurdo, P. Capezzuto, and G. Bruno, "Wet chemical treatment in hydrazine-sulfide solutions for sulfide and nitride monomolecular surface films on gaas(100)," *Journal of the Electrochemical Society*, vol. 152, no. 5, pp. 2–6, 2005.

[48] K. Lahlil, D. Paget, V. L. Berkovits, G. Monier, P. Dumas, F. Ozanam, V. P. Ulin, L. Bideux, and S. Kubsky, "Real time infra-red absorption analysis of nitridation of gaas(001) by hydrazine solutions," *Journal of the Electrochemical Society*, vol. 160, no. 4, pp. 229–236, 2013.

[49] V. L. Berkovits, T. V. L'vova, and V. P. Ulin, "Nitride chemical passivation of a gaas (100) surface: Effect on the electrical characteristics of au/gaas surface-barrier structures," *Semiconductors*, vol. 45, no. 12, pp. 1575–1579, 2011.

[50] V. Berkovits, A. Gordeeva, T. L'vova, V. Ulin, G. Iluridze, T. Minashvili, P. J. Kervalishvili, and A. Gigineishvili, *Nuclear Radiation Nanosensors and Nanosensory Systems, Chapter 6: Nitride and Sulfide Chemisorbed Layers as the Surface Passivants for A^3B^5 Semiconductors*. Springer, 2016.

[51] T. V. L'vova, V. L. Berkovits, M. S. Dunaevski, V. M. Lantratov, I. V. Makarenko, and V. P. Ulin, "Wet chemical nitridation of (100)gaas surface: Effect on electrical parameters of surface-barrier au-ti/gaas structures," *Semiconductors*, vol. 37, no. 8, pp. 955–959, 2003.

[52] J. Riikonen, J. Sormunen, H. Koskenvaara, M. Mattila, M. Sopanen, and H. Lipsanen, "Passivation of gaas surface by ultrathin epitaxial gan layer," *Journal of Crystal Growth*, vol. 272, no. 1-4, pp. 621–626, 2004.

[53] H. Vilchis, V. M. Sanchez-R., and A. Escobosa, "Cubic gan layers grown by metalorganic chemical vapor deposition on gan templates obtained by nitridation of gaas," *Thin Solid Films*, vol. 520, no. 16, pp. 5191–5194, 2012.

[54] H. Okumura, S. Misawa, and S. Yoshida, "Epitaxial growth of cubic and hexagonal gan on gaas by gas-source molecular-beam epitaxy," *Applied Physics Letters*, vol. 59, no. 9, pp. 1058–1060, 1991.

[55] M. Ambrico, M. Losurdo, P. Capezzuto, G. Bruno, T. Ligonzo, L. Schiavulli, I. Farella, and V. Augelli, "A study of remote plasma nitrided ngaas/au schottky barrier," *Solid-State Electronics*, vol. 49, no. 3, pp. 413–419, 2005.

[56] M. Losurdo, P. Capezzuto, G. Bruno, G. Leo, and E. A. Irene, "Iii–v surface plasma nitridation: A challenge for iii–v nitride epigrowth," *Journal of Vacuum Science & Technology A*, vol. 17, no. 4, pp. 2194–2201, 2002.

[57] M. Ambrico, M. Losurdo, P. Capezzuto, G. Bruno, T. Ligonzo, and H. Haick, "Probing electrical properties of molecule-controlled or plasma-nitrided GaAs surfaces: Two different tools for modifying the electrical characteristics of metal/GaAs diodes," *Applied Surface Science*, vol. 252, no. 21, pp. 7636–7641, 2006.

[58] P. A. Alekseev, M. S. Dunaevskiy, G. E. Cirlin, R. R. Reznik, A. N. Smirnov, D. A. Kirilenko, V. Y. Davydov, and V. L. Berkovits, "Unified mechanism of the surface fermi level pinning in iii-as nanowires," *Nanotechnology*, vol. 39, no. 31, pp. 1–9, 2018.

[59] W. E. Spicer, I. Lindau, P. Skeath, C. Y. Su, and P. Chye, "Unified mechanism for schottky-barrier formation and iii-v oxide interface states," *Physical Review Letters*, vol. 44, no. 6, pp. 420–423, 1980.

[60] T. T. Chiang and W. E. Spicer, "Arsenic on gaas: Fermi-level pinning and thermal desorption studies," *Journal of Vacuum Science & Technology A: Vacuum, Surfaces, and Films*, vol. 7, no. 3, pp. 724–730, 2002.

[61] S. Anantathanasarn and H. Hasegawa, "Photoluminescence and capacitance–voltage characterization of gaas surface passivated by an ultrathin gan interface control layer," *Applied Surface Science*, vol. 190, no. 1, pp. 343–347, 2002.

[62] M. Scharber and N. Sariciftci, "Efficiency of bulk-heterojunction organic solar cells," *Progress in Polymer Science*, vol. 38, no. 12, pp. 1929–1940, 2013.

[63] H. J. Snaith, "Perovskites: The emergence of a new era for low-cost, high-efficiency solar cells," *The Journal of Physical Chemistry Letters*, vol. 4, no. 21, p. 3623–3630, 2013.

[64] J. Y. Kim, K. Lee, N. E. Coates, D. Moses, T.-Q. Nguyen, M. Dante, and A. J. Heeger, "Efficient tandem polymer solar cells fabricated by all-solution processing," *Advanced Materials*, vol. 317, no. 5835, pp. 222–225, 2010.

[65] B. C. Thompson and J. M. J. Fréchet, "Polymer–fullerene composite solar cells," *Angewandte Chemie International Edition*, vol. 47, no. 1, pp. 58–77, 2007.

[66] C. J. Brabec, S. Gowrisanker, J. J. M. Halls, D. Laird, S. Jia, and S. P. Williams, "Polymer–fullerene bulk-heterojunction solar cells," *Advanced Materials*, vol. 22, no. 34, pp. 3839–3856, 2010.

[67] H. J. Joyce, C. J. Docherty, Q. Gao, H. H. Tan, C. Jagadish, J. Lloyd-Hughes, L. M. Herz, and M. B. Johnston, "Electronic properties of gaas, inas and inp nanowires studied by terahertz spectroscopy," *Nanotechnology*, vol. 24, no. 21, pp. 1–7, 2013.

[68] Nobel Media AB 2019, "Press release". NobelPrize.org, 2019. <https://www.nobelprize.org/prizes/chemistry/2000/press-release/>.

[69] S. Zhang, G. Li, Y. Yang, Y. Wu, H.-Y. Chen, R. I. Chen, and J. Hou, "Synthesis of a low band gap polymer and its application in highly efficient polymer solar cells," *Journal of the American Chemical Society*, vol. 131, no. 43, pp. 15586–15587, 2009.

[70] Y. Yang, Y. Lee, Y. Lee, C. Chiang, C. Shen, C. Wu, Y. Ohta, T. Yokozawa, and C. Dai, "Synthesis and characterization of poly(3-hexylthiophene)–poly(3-hexyloxythiophene) random copolymers with tunable band gap via grignard metathesis polymerization," *Polymer International*, vol. 6, no. 12, pp. 2068–2075, 2014.

[71] J. Hou, T. L. Chen, S. Zhang, L. Huo, S. Sista, and Y. Yang, "An easy and effective method to modulate molecular energy level of poly(3-alkylthiophene) for high-v_{oc} polymer solar cells," *Macromolecules*, vol. 42, no. 23, pp. 9217–9219, 2009.

[72] X. Hu and L. Xu, "Structure and properties of 3-alkoxy substituted polythiophene synthesized at low temperature," *Polymer*, vol. 41, no. 26, pp. 9147–9154, 2000.

[73] G. Koeckelberghs, M. Vangheluw, K. Van Doorsselaere, E. Robijns, A. Persoons, and T. Verbiest, "Regioregularity in poly(3-alkoxythiophene)s: Effects on the faraday rotation and polymerization mechanism," *Macromolecular Rapid Communications*, vol. 27, no. 22, pp. 1920–1925, 2006.

[74] C. S. A. P. Guy Koeckelberghs, Marnix Vangheluwe and T. Verbiest, "Regioregular poly(3-alkoxythiophene)s: Toward soluble, chiral conjugated polymers with a stable oxidized state," *Advanced Materials*, vol. 38, no. 13, pp. 5554–5559, 2005.

[75] W. Zhang, S. Lehmann, K. Mergenthaler, J. Wallentin, M. T. Borgstrom, M. E. Pistol, and A. Yartsev, "Carrier recombination dynamics in sulfur-doped inp nanowires," *Nano Lett*, vol. 15, no. 11, pp. 7238–44, 2015.

[76] O. Demichel, M. Heiss, J. Bleuse, H. Mariette, and A. Fontcuberta i Morral, "Impact of surfaces on the optical properties of gaas nanowires," *Applied Physics Letters*, vol. 97, no. 20, 2010.

[77] S. Munch, S. Reitzenstein, M. Borgstrom, C. Thelander, L. Samuelson, L. Worschech, and A. Forchel, "Time-resolved photoluminescence investigations on hfo2-capped inp nanowires," *Nanotechnology*, vol. 21, no. 10, p. 105711, 2010.

[78] L. M. Smith, H. E. Jackson, J. M. Yarrison-Rice, and C. Jagadish, "Insights into single semiconductor nanowire heterostructures using time-resolved photoluminescence," *Semiconductor Science and Technology*, vol. 25, no. 2, pp. 1–13, 2010.

[79] H. Photonics, "Guide to streak cameras," 2008. `https://www.hamamatsu.com/resources/pdf/sys/SHSS0006E_STREAK.pdf`, Last accessed on 2019-03-05.

[80] H. J. Joyce, Q. Gao, H. H. Tan, C. Jagadish, Y. Kim, X. Zhang, Y. Guo, and J. Zou, "Twin-free uniform epitaxial gaas nanowires grown by a two-temperature process," *Nano Letters*, vol. 7, no. 4, pp. 921–926, 2007.

[81] N. Jiang, J. Wong-Leung, H. J. Joyce, Q. Gao, H. H. Tan, and C. Jagadish, "Understanding the true shape of au-catalyzed gaas nanowires," *Nano Lett*, vol. 14, no. 10, pp. 5865–5872, 2014.

[82] S. Lehmann, D. Jacobsson, and K. A. Dick, "Crystal phase control in gaas nanowires: opposing trends in the ga- and as-limited growth regimes," *Nanotechnology*, vol. 26, no. 30, p. 1–7, 2015.

[83] D. Jacobsson, F. Panciera, J. Tersoff, M. C. Reuter, S. Lehmann, S. Hofmann, K. A. Dick, and F. M. Ross, "Interface dynamics and crystal phase switching in gaas nanowires," *Nature*, vol. 531, p. 317–322, 2016.

[84] H. J. Joyce, Q. Gao, H. H. Tan, C. Jagadish, Y. Kim, M. A. Fickenscher, S. Perera, T. B. Hoang, L. M. Smith, H. E. Jackson, J. M. Yarrison-Rice, X. Zhang, and J. Zou, "Unexpected benefits of rapid growth rate for iii-v nanowires," *Nano Letters*, vol. 9, no. 2, pp. 695–701, 2009.

[85] S. A. Dayeh, E. T. Yu, and D. Wang, "Iii−v nanowire growth mechanism: V/iii ratio and temperature effects," *Nano Letters*, vol. 7, no. 8, pp. 2486–2490, 2007.

[86] K. A. Dick, P. Caroff, J. Bolinsson, M. E. Messing, J. Johansson, K. Deppert, L. R. Wallenberg, and L. Samuelson, "Control of iii–v nanowire crystal structure by growth parameter tuning," *Semiconductor Science and Technology*, vol. 25, no. 2, pp. 1–11, 2010.

[87] K. A. Dick, P. Caroff, J. Bolinsson, M. E. Messing, J. Johansson, K. Deppert, L. R. Wallenberg, and L. Samuelson, "Why does wurtzite form in nanowires of iii-v zinc blende semiconductors?," *Physical Review Letters*, vol. 99, no. 14, pp. 1–4, 2007.

[88] P. Caroff, K. A. Dick, J. Johansson, M. E. Messing, K. Deppert, and L. Samuelson, "Controlled polytypic and twin-plane superlattices in iii–v nanowires," *Nature Nanotechnology*, vol. 4, p. 50–55, 2009.

[89] V. Dhaka, A. Perros, S. Naureen, N. Shahid, H. Jiang, J.-P. Kakko, T. Haggren, E. Kauppinen, A. Srinivasan, and H. Lipsanen, "Protective capping and surface passivation of iii-v nanowires by atomic layer deposition," *AIP Advances*, vol. 6, no. 1, pp. 1–7, 2016.

[90] *Fiji F200 ALD System Installation and Use Manual.* Cambridge, MA: Cambridge NanoTech Inc., 2008. `https://is.muni.cz/el/1431/jaro2017/F4280/um/69248846/69248852/FIJI_F200_ALD.pdf`.

[91] C. Shi, Y. Yao, Y. Yang, and Q. Pei, "Regioregular copolymers of 3-alkoxythiophene and their photovoltaic application," *Journal of the American Chemical Society*, vol. 128, no. 27, pp. 8980–8986, 2006.

[92] E. E. Sheina, S. M. Khersonsky, E. G. Jones, and R. D. McCullough, "Highly conductive, regioregular alkoxy-functionalized polythiophenes: A new class of stable, low band gap materials," *Chemistry of Materials*, vol. 17, no. 13, pp. 3317–3319, 2005.

[93] S. Vandeleene, K. V. den Bergh, T. Verbiest, and G. Koeckelberghs, "Influence of the polymerization methodology on the regioregularity and chiroptical properties of poly(alkylthiothiophene)s," *Macromolecules*, vol. 41, no. 14, pp. 5123–5131, 2008.

[94] H. C. Casey and F. Stern, "Concentration-dependent absorption and spontaneous emission of heavily doped gaas," *Journal of Applied Physics*, vol. 47, no. 2, pp. 631–643, 1976.

[95] Y. P. Varshni, "Temperature dependence of the energy gap in semiconductors," *Physica*, vol. 34, no. 1, pp. 149–154, 1967.

[96] S. M. Sze and K. K. Ng, *Physics of Semiconductor Devices, 3rd Edition.* Hoboken, NJ, USA: John Wiley & Sons, Inc., 2007.

[97] V. Alperovich, O. Tereshchenko, N. Rudaya, D. Sheglov, A. Latyshev, and A. Terekhov, "Surface passivation and morphology of gaas(100) treated in hcl-isopropanol solution," *Applied Surface Science*, vol. 235, no. 3, p. 249–259, 2004.

[98] O. E. Tereshchenko, S. I. Chikichev, and A. S. Terekhov, "Composition and structure of hcl-isopropanol treated and vacuum annealed gaas(100) surfaces," *Journal of Vacuum Science & Technology A*, vol. 17, no. 5, pp. 2655–2662, 1999.

Chapter 5

Appendix

	A	B	C	D	E	F	G
1	Combined N2 + H2 Final						
2	Task	Operation	Value				
3	Flow	0	40		Stabilize	12	
4	Flow	1	20		Stabilize	13	
5	MFC Valve	4	1		Stabilize	14	
6	Heater	12	250		Stabilize	15	
7	Heater	13	250		Flow	0	20
8	Heater	14	250		Flow	1	0
9	Heater	15	250		Flow	2	133
10	Wait		300/3600		Flow	4	4
11	Stabilize	12			Wait		20
12	Stabilize	13			Plasma		300
13	Stabilize	14			***Wait***		***10/20/40***
14	Stabilize	15			Plasma		0
15	Flow	0	40		Wait		30
16	Flow	1	200		Flow	2	0
17	Flow	4	20		Flow	4	0
18	Wait		20		MFC Valve	2	0
19	Plasma		300		MFC Valve	4	0
20	***Wait***		***3/6***		Flow	0	10
21	Plasma		0		Flow	1	20
22	Wait		30		Heater	12	200
23	Flow	4	0		Heater	13	200
24	MFC Valve	2	1		Heater	14	200
25	Heater	12	250		Heater	15	200
26	Heater	13	250		Door Purge		1
27	Heater	14	250				
28	Heater	15	360				

Figure 5.1: Excel spreadsheet listing every step in the plasma process used by the Fiji F200. This recipe is saved on the machine's computer as well.

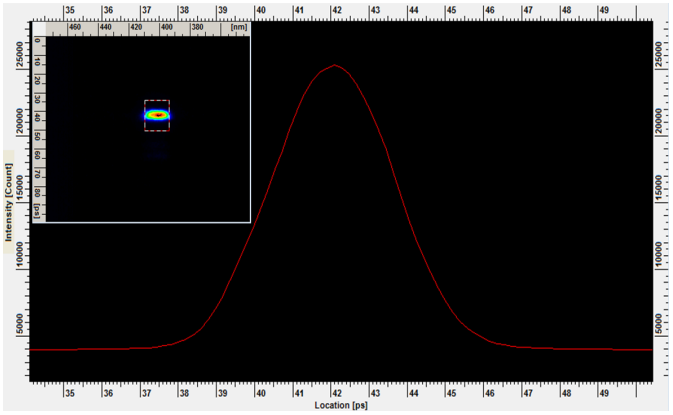

Figure 5.2: TRPL spectra demonstrating how the streak camera resolves a 100 fs laser pulse. Temporal resolution is about 4 ps.

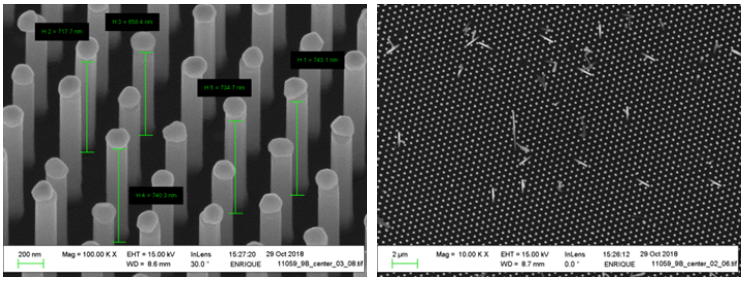

(a) (b)

Figure 5.3: SEM images of nanowire array at the center of sample 11059. a) View at angle = 30°, magnification = 100,000x b) Top view at magnification = 10,000x

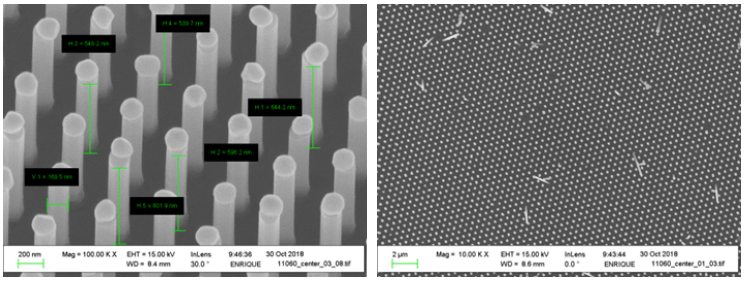

(a) (b)

Figure 5.4: SEM images of nanowire array at the center of sample 11060. a) View at angle = 30°, magnification = 100,000x b) Top view at magnification = 10,000x

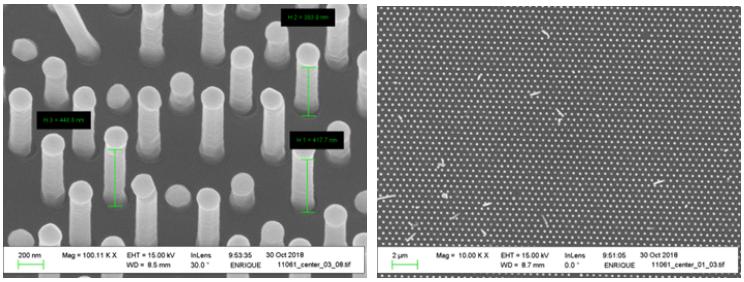

(a) (b)

Figure 5.5: SEM images of nanowire array at the center of sample 11061. a) View at angle = 30°, magnification = 100,000x b) Top view at magnification = 10,000x

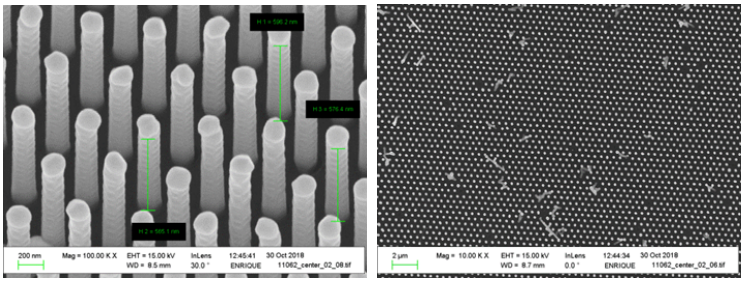

(a) (b)

Figure 5.6: SEM images of nanowire array at the center of sample 11062. a) View at angle = 30°, magnification = 100,000x b) Top view at magnification = 10,000x

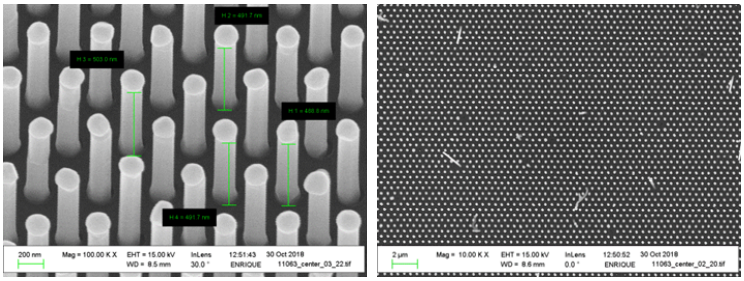

(a) (b)

Figure 5.7: SEM images of nanowire array at the center of sample 11063. a) View at angle = 30°, magnification = 100,000x b) Top view at magnification = 10,000x

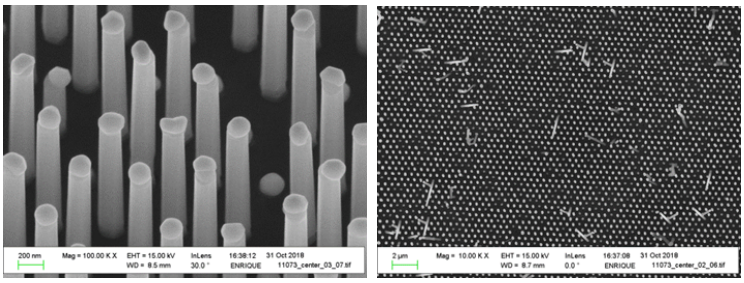

(a) (b)

Figure 5.8: SEM images of nanowire array at the center of sample 11073. a) View at angle = 30°, magnification = 100,000x b) Top view at magnification = 10,000x

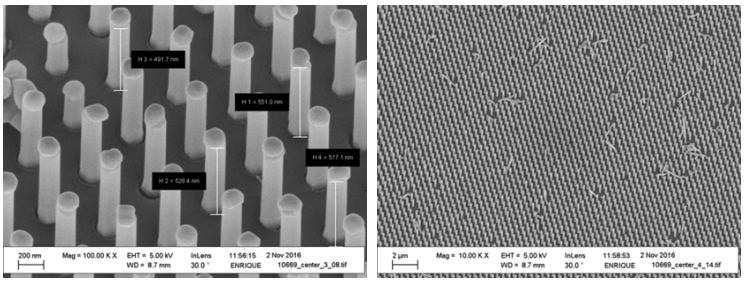

(a) (b)

Figure 5.9: SEM images of nanowire array at the center of sample 10669. a) View at angle = 30°, magnification = 100,000x b) Top view at magnification = 10,000x

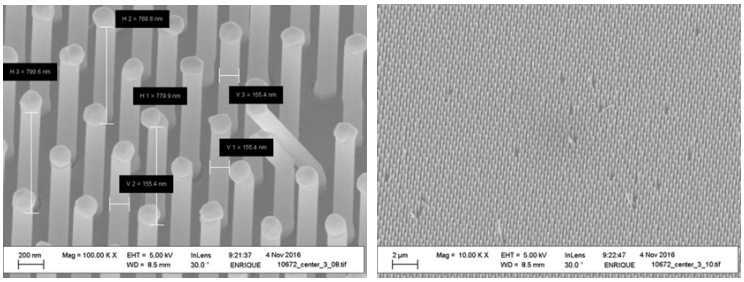

(a) (b)

Figure 5.10: SEM images of nanowire array at the center of sample 10672. a) View at angle = 30°, magnification = 100,000x b) Top view at magnification = 10,000x

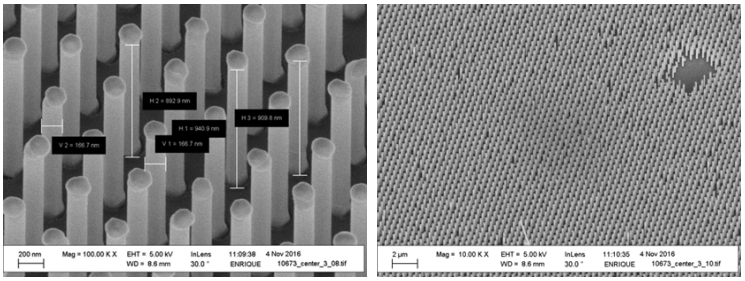

(a) (b)

Figure 5.11: SEM images of nanowire array at the center of sample 10673. a) View at angle = 30°, magnification = 100,000x b) Top view at magnification = 10,000x

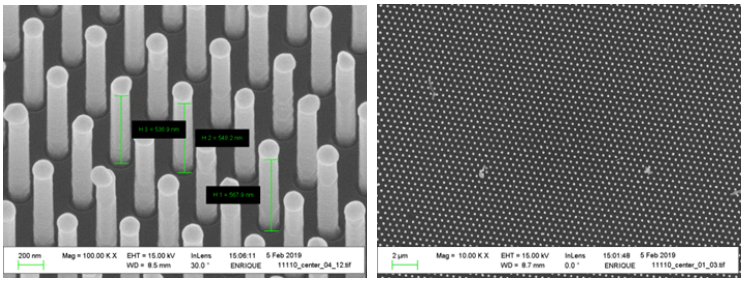

(a) (b)

Figure 5.12: SEM images of nanowire array at the center of sample 11110. a) View at angle = 30°, magnification = 100,000x b) Top view at magnification = 10,000x

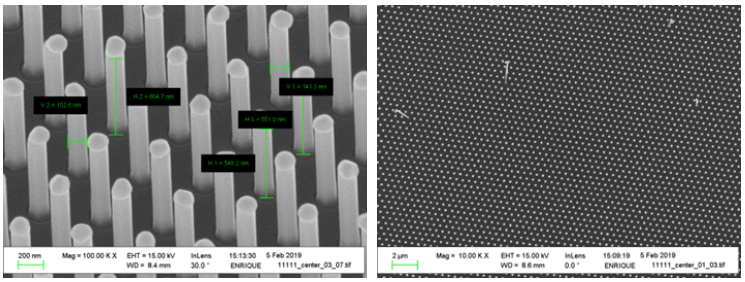

(a) (b)

Figure 5.13: SEM images of nanowire array at the center of sample 11111. a) View at angle = 30°, magnification = 100,000x b) Top view at magnification = 10,000x